

Morphology and distribution of fossil soils in the Permo-Pennsylvanian Wichita and Bowie Groups, north-central Texas, USA: implications for western equatorial Pangean palaeoclimate during icehouse–greenhouse transition

NEIL JOHN TABOR* and ISABEL P. MONTAÑEZ†

**Department of Geological Sciences, Southern Methodist University, Dallas, TX 75275, USA (E-mail: ntabor@mail.smu.edu)*

†*Department of Geology, University of California, Davis, CA 95616, USA*

ABSTRACT

Analysis of stacked Permo-Pennsylvanian palaeosols from north-central Texas documents the influence of palaeolandscape position on pedogenesis in aggradational depositional settings. Palaeosols of the Eastern shelf of the Midland basin exhibit stratigraphic trends in the distribution of soil horizons, structure, rooting density, clay mineralogy and colour that record long-term changes in soil-forming conditions driven by both local processes and regional climate. Palaeosols similar to modern histosols, ultisols, vertisols, inceptisols and entisols, all bearing morphological, mineralogical and chemical characteristics consistent with a tropical, humid climate, represent the Late Pennsylvanian suite of palaeosol orders. Palaeosols similar to modern alfisols, vertisols, inceptisols, aridisols and entisols preserve characteristics indicative of a drier and seasonal tropical climate throughout the Lower Permian strata. The changes in palaeosol morphology are interpreted as being a result of an overall climatic trend from relatively humid and tropical, moist conditions characterized by high rainfall in the Late Pennsylvanian to progressively drier, semi-arid to arid tropical climate characterized by seasonal rainfall in Early Permian time. Based on known Late Palaeozoic palaeogeography and current hypotheses for atmospheric circulation over western equatorial Pangea, the Pennsylvanian palaeosols in this study may be recording a climate that is the result of an orographic control over regional-scale atmospheric circulation. The trend towards a drier climate interpreted from the Permian palaeosols may be recording the breakdown of this pre-existing orographic effect and the onset of a monsoonal atmospheric circulation system over this region.

Keywords Late Palaeozoic palaeoclimate, palaeosols, Permo-Carboniferous.

INTRODUCTION

Outcrop and numerically based modelling studies of the Late Palaeozoic geological record indicate that Earth's climate system underwent significant evolutionary change during this period. It is generally believed that climate change occurred in response to the formation of the supercontinent Pangea, an accompanying trans-

ition from icehouse to greenhouse states and a probable global-scale reorganization of atmospheric circulation systems (Rowley *et al.*, 1985; Cecil, 1990; Parrish, 1993; West *et al.*, 1997; Gibbs *et al.*, 2002; and references therein). This plethora of studies indicates that the mid-latitude and equatorial regions of Pangea became progressively more arid, with more seasonal precipitation, throughout the Late Palaeozoic,

strongly supporting the development of northern hemisphere monsoonal circulation during this interval. Furthermore, it has been hypothesized that monsoonal circulation began in the Late Carboniferous and reached its peak in the Middle Triassic based primarily upon lithological and palaeontological studies of North American and European terrestrial strata (Parrish, 1993).

Geological proxy records (e.g. coals, evaporites, aeolianites, tillites) and numerical models can provide an excellent framework for the long-term development of climate systems over Pangea. Few detailed records exist, however, that offer insight into higher resolution spatial and temporal variations in climate regimes that accompanied the evolution of Pangean monsoonal circulation. Significantly, recent studies of terrestrial deposits and their associated palaeosols in the south-west USA suggest that monsoonal circulation was well-established over western equatorial Pangea by earliest Permian time (Kessler *et al.*, 2001; Soreghan G.S. *et al.*, 2002; Soreghan M.J. *et al.*, 2002; Tabor & Montañez, 2002). These studies, coupled with continuing discrepancies in model-data comparisons for low-latitude Pangea (Patzkowsky *et al.*, 1991; Rees *et al.*, 2001; Gibbs *et al.*, 2002), highlight the necessity of understanding the evolution of specific Pangean climate zones.

The palaeosol-rich, Permo-Pennsylvanian terrestrial strata of north-central Texas hold the potential to provide insight into climate change over low-latitude Pangea, given that climate variation would have been most pronounced in western equatorial Pangea because of the configuration of the supercontinent and its attendant effects on atmospheric circulation and precipitation patterns (Dubiel *et al.*, 1991; Parrish, 1993). Furthermore, rich faunal and floral collections and interstratified regionally correlatable fluvial sandstone bodies and fusulinid-bearing limestones provide a chronostratigraphic framework in which to define spatial and temporal trends in palaeosol morphology, mineralogy and geochemistry and the degree of palaeopedogenic development. This study evaluates the influence of local- to regional-scale autogenic and larger scale allogenic processes on the stratigraphic distribution of palaeosol morphologies and compositions through detailed field, petrographic, mineralogical and geochemical analyses of ≈ 200 Permo-Pennsylvanian palaeosols. These palaeosols provide a detailed data set for comparison with previously published palaeoclimate trends based on geological data and numerical models. The

results of this study help to refine the nature and timing of climate change in western equatorial Pangea during the early stages of supercontinent formation, major change in global atmospheric circulation and the onset of deglaciation.

GEOLOGICAL SETTING

The study area in north-central Texas (Fig. 1) was located in the western coastal zone of equatorial Pangea during the Late Palaeozoic (Ziegler *et al.*, 1997) and remained between 0 and 5°N of the equator throughout this time period (Golonka *et al.*, 1994; Scotese, 1999; Loope *et al.*, 2004). Major tectonic elements such as the Muenster Arch and the Wichita, Arbuckle and Ouachita Mountains (Fig. 1) had developed by latest Pennsylvanian time (Oriol *et al.*, 1967), and tectonic quiescence has characterized the region since (Donovan *et al.*, 2001). Late Pennsylvanian (Virgilian) and Early Permian (Wolfcampian and Leonardian) terrestrial strata of north-central Texas, along with subordinate marine sediments, were deposited upon the broad, gently sloping Eastern shelf of the Midland basin as it subsided throughout the Late Palaeozoic (Fig. 1; Brown *et al.*, 1987; Hentz, 1988). A minor component of detrital sediments representing the Upper Pennsylvanian and Lower Permian strata of the Eastern Midland basin may have been derived from Early Palaeozoic sediments and metamorphic rocks of the distal Ouachita and Arbuckle Mountain chains (Hentz, 1988). However, the principal source of detrital sediments during this time was probably derived from second-cycle terrigenous-clastic sediments from Middle Pennsylvanian fan-delta and fluvial facies that were eroded from the proximal Ouachita foldbelt and Muenster Highlands (Fig. 1; Brown, 1973). Although there is no evidence for a major change in the lithology of source lands during Permo-Pennsylvanian deposition, a progressive decrease upsection in grain size and thickness of fluvial sandstones, coupled with a decrease in stratigraphic frequency of thick, multistorey sandstones, is interpreted as recording significant denudation of the source areas by the close of the Early Permian (Hentz, 1988).

The primarily terrestrial deposits of the Bowie and Wichita Groups on the north-eastern portion of the Eastern shelf reach a thickness of up to 530 m in the east and thin westward towards marine-dominated strata (Fig. 2). Three terrestrial facies are recognized in the Late Pennsylvanian

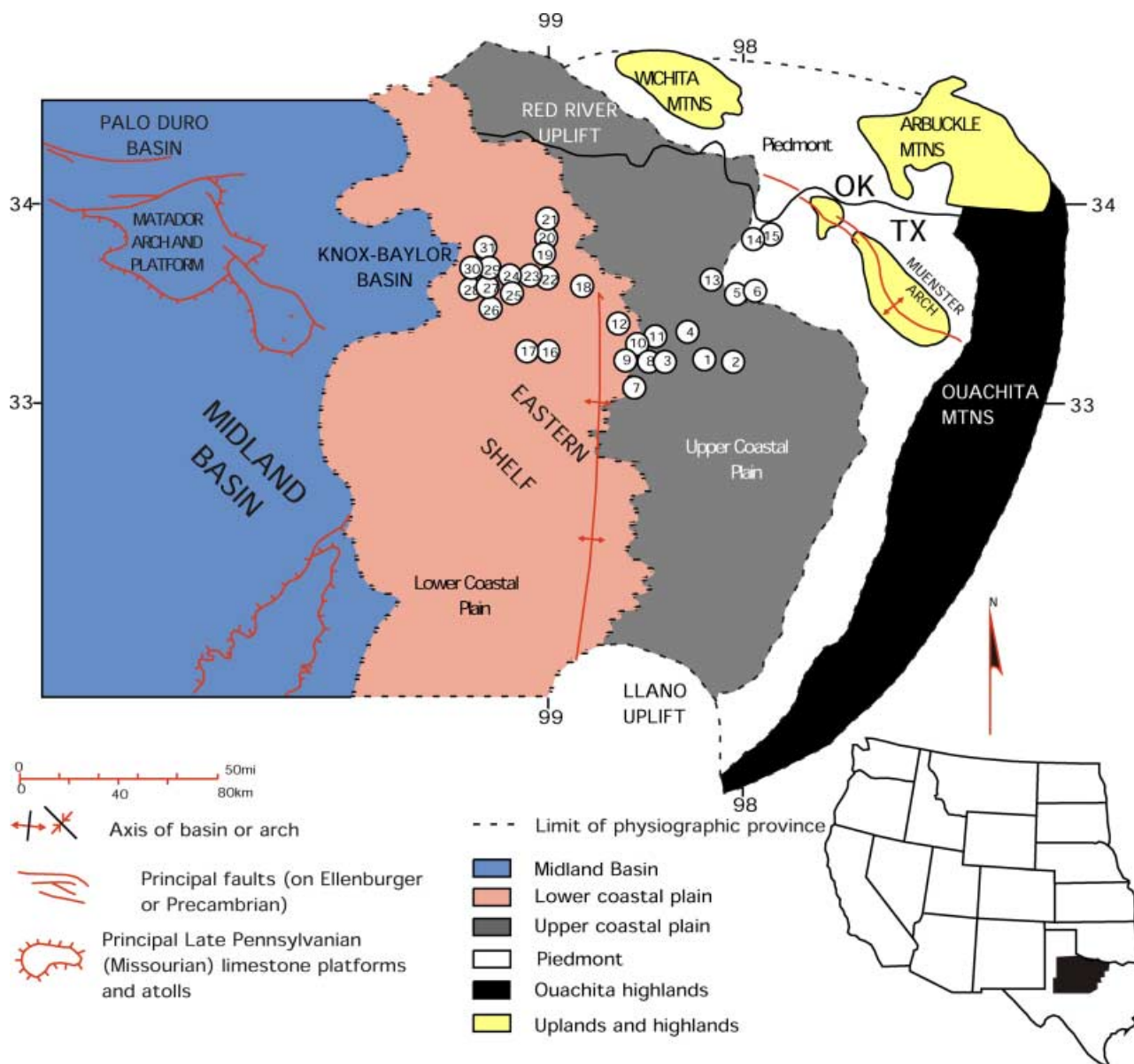


Fig. 1. Regional distribution of source terranes and physiographic provinces in the latest Pennsylvanian to Early Permian, Eastern Shelf of the Midland Basin. Province boundaries are defined for the period of maximum regression in the earliest Permian. Structural and tectonic elements shown are for the pre-Virgilian palaeogeography of north-central Texas; the Muenster and Ouachita highlands remained significant topographic features in the Early Permian. Encircled numbers delineate locations of palaeosol-bearing stratigraphic sections used in this study. Diagram modified after Brown *et al.* (1987) and Hentz (1988).

and Early Permian terrestrial strata of the Eastern Midland basin: (1) sand- and gravel-rich channel-bar facies; (2) point-bar facies; and (3) floodplain facies (Hentz, 1988). Sand and gravel-rich, channel-bar facies were deposited by braided stream systems fringing the north-eastern highlands, whereas the point-bar facies record penecontemporaneous meandering stream systems that developed on the Eastern shelf to the south and west of the braided stream system.

Alluvial floodplain deposits formed primarily in association with meandering streams given their stratigraphic predominance in the western and southern portions of the study area. Based on regional facies distributions, Hentz (1988) defined three physiographic provinces for the latest Pennsylvanian to Early Permian landscape of the Eastern shelf: (1) the piedmont province dominated by sand- and gravel-rich channel-bar facies and, to a lesser degree, point-bar facies; (2)

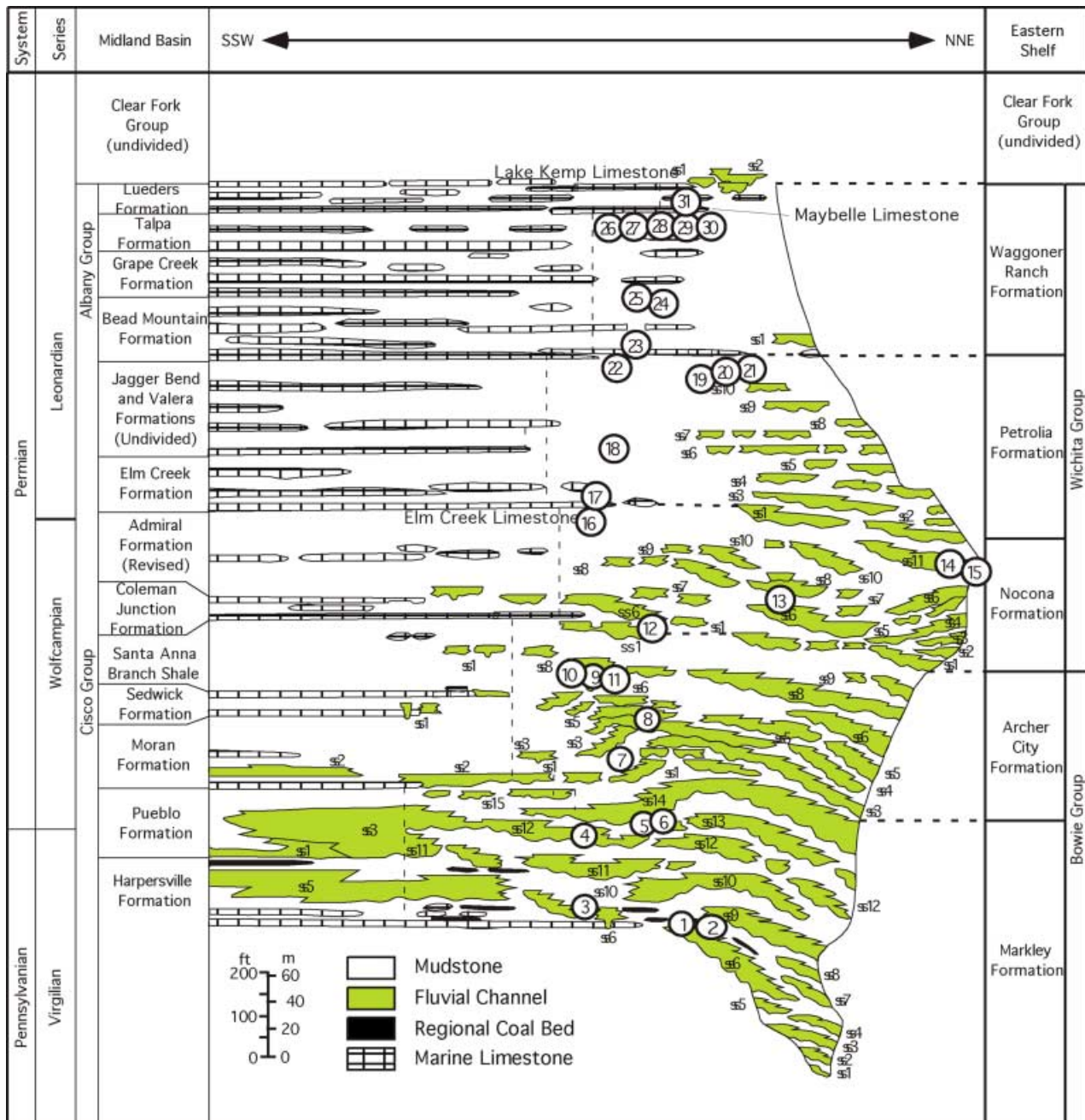


Fig. 2. Regional correlation of Late Pennsylvanian and Early Permian strata in north-central Texas. Light grey beds delineate regionally extensive fluvial sandstone sets; black horizons are coals; white regions represent alluvial mudstones and intercalated siltstones and thin-bedded, fine-grained sandstones; dark grey beds are marine limestones. Encircled numbers show the stratigraphic distribution of studied palaeosols – numbers correspond to sites in Fig. 1. Diagram modified after Hentz (1988).

the upper coastal plain province characterized by point-bar facies; and (3) the lower coastal plain province dominated by floodplain facies and, to a lesser degree, point-bar facies.

A high-resolution chronostratigraphic framework for Permo-Pennsylvanian terrestrial strata of north-central Texas has been developed

through correlation of multiple fusulinid-bearing limestones and intercalated multistorey fluvial sandstone deposits, which were described (ss units in Fig. 2) and regionally correlated by Hentz (1988). The Pennsylvanian–Permian boundary (301 ± 2 Ma; Rasbury *et al.*, 1998) occurs within a few metres of the contact

between the Markley and Archer City Formations of the Bowie Group (Dunbar & Committee on Stratigraphy, 1960). The Wolfcampian–Leonardian boundary (283 ± 2 Ma; Ross *et al.*, 1994) is defined by the fusulinid-bearing Elk City Limestone at the base of the Petrolia Formation of the Wichita Group (Fig. 2).

BURIAL HISTORY

The entire stratigraphic thickness of the Late Pennsylvanian and Early Permian rocks in the study area is ≈ 1250 m, with the lower 1000 m dominated by sedimentary rocks characteristic of terrestrial depositional facies (Hentz, 1988; Nelson *et al.*, 2001; Tabor & Montañez, 2002). Deposition in this area during the Triassic and Jurassic was insignificant (Oriol *et al.*, 1967; McGowen *et al.*, 1979). However, Cretaceous strata were probably deposited in the area, as shown by outliers of Cretaceous marine rocks in the extreme western portion of the study area, but these probably did not exceed 330 m in thickness (Barnes *et al.*, 1987). Tertiary and early Quaternary burial was insignificant in this area (Barnes *et al.*, 1987). Therefore, the maximum burial depth of Virgilian strata in the Eastern Midland basin probably did not exceed 1600 m in thickness. This shallow burial history is reflected by relatively mild burial temperatures that never exceeded 40–45 °C in the Early Permian strata along the flanks of the Midland basin (Bein & Land, 1983).

METHODS

Thirty-one stratigraphic sections were dug or picked back 30–60 cm to provide a fresh surface for description and sampling. The geographic and stratigraphic positions of these 31 sites are shown in Figs 1 and 2. Palaeosols ($n = 190$) from the 31 stratigraphic sections of the Bowie and Wichita Groups were logged and described in detail within the chronostratigraphic and sedimentological framework defined by Hentz (1988). Palaeosol profiles were recognized and described using established criteria (Retallack, 1988; Kraus & Aslan, 1993; Kraus, 1999). Profile tops were identified on the basis of a marked change in grain size and/or colour, as well as preservation of primary sedimentary structures. Profile bases were delineated at the lowest occurrence of unaltered parent material. Palaeosol and sedi-

ment colours were identified from dry samples using Munsell colour charts (Munsell Color, 1975). Palaeosol classification primarily follows the USDA Soil Taxonomy system (Soil Survey Staff, 1975, 1998).

Palaeosol matrix was sampled at 0.1–0.2 m vertical spacings; rhizoliths and nodules were sampled where present in the profile. Palaeosol matrix samples were disaggregated overnight by ultrasonic agitation in a dilute Na_2CO_3 solution and analysed for grain-size distribution. Percentage sand, silt and clay was determined by centrifugation and filtration. Thin sections ($n = 78$) of representative samples were examined for their micromorphology and mineralogy according to the approaches and terminology of Brewer (1976) and Wright (1990).

X-ray diffraction of the $< 2 \mu\text{m}$ size fraction was carried out for identification of clay mineralogy. Samples were exchange saturated with K or Mg on filter membranes and transferred to glass slides as oriented aggregates. A split of the Mg-saturated clays was also treated with glycerol. Oriented aggregates of all Mg-treated samples were analysed at 25 °C. K-treated samples were analysed at 25 °C, 300 °C and 500 °C after 2 h of initial heating at their respective temperatures. Step scan analyses were performed on a Diano 8500 X-ray diffractometer with $\text{CuK}\alpha$ radiation between 2 and $30^\circ 2\theta$ with a step size of $0.04^\circ 2\theta$ and a 1 s count time.

PALAEOSOL TYPES AND PALAEOENVIRONMENTAL IMPLICATIONS

Field-scale indicators of pedogenesis in the studied Permo-Pennsylvanian terrestrial strata include colour, mottling, structure, slickensides, accumulation of oxides, clays and carbonate and fossil root traces. Palaeosol profiles were subdivided into horizons on the basis of downprofile changes in macro- and micromorphological features, clay mineralogy and abundance and geochemical characteristics. Eight major pedotypes (*sensu* Retallack, 1994; Table 1; Figs 3 and 4) are recognized based on distinctive characteristics that include the aforementioned macromorphological features as well as profile thickness, degree of development (maturity), relationship to stratigraphically adjacent palaeosols (i.e. composite, compound or cumulate palaeosols; *sensu* Marriott & Wright, 1993; Kraus, 1999) and clay mineralogy. Palaeosols assigned to each pedotype are

Table 1. Morphology, mineralogy and chemical indices of representative profiles of pedotypes.

Pedotype and stratigraphic occurrence	Horizon depth (m)*	Macromorphology	Type profile variation	Nodule and rhizolith mineralogy†	≤ 2 μm Clay mineralogy‡	Province
A: Histosol Markley Fm.	Oi (0–0.20) Aj (0.20–0.27)	Dark grey to black, massive and organic-rich claystone. Whole <i>Neuropteris</i> leaves. Non-calcareous. Light grey (5Y 7/1) claystone with fine granular structure. Common medium to coarse yellow (5Y 8/8) mottles. Dense network of thin (< 1 cm), tabular yellow (5Y 8/8) rhizoliths. Non-calcareous.	Organic layers variable thickness (3–70 cm); thin clastic partings common. Rare jarosite replacement of rhizoliths.	– Jarosite (40%)	– K, I (62%)	Lower coastal
B: Ultisol Markley Fm.	C (0.27–0.35) ABt1 (0–0.15) Bt2 (0.15–0.60) BCg(0.60–1.02)	Grey (5Y 6/1), massive silty claystone. Non-calcareous. Red (10R 4/4) claystone with granular to subangular blocky structure. Common discrete, fine-scale yellow (5Y 8/6) vermicular mottles. Abundant Fe- (less so Mn-) oxide coatings and oriented clay skins on matrix aggregates. Non-calcareous. Red (10R 4/3) claystone with subangular blocky structure. Few discrete, fine-scale yellow (10YR 8/8) subspherical mottles. Abundant Fe- (less so Mn-) oxide coatings and oriented clay skins. Non-calcareous. Mottled grey (5Y 6/1) and red (10R 4/4) silty claystone with subangular blocky structure. Discrete, brown-yellow (10YR 6/8) to red (5R 4/8) vertically oriented tubular mottles and nodules. Non-calcareous.	Clay accumulation in upper profiles varies from moderate to significant.	– –	K, I (59%) K, I (67%) K, I (78%) K, I (42%)	Lower coastal

Table 1. (Continued).

Pedotype and stratigraphic occurrence	Horizon depth (m)*	Macromorphology	Type profile variation	Nodule and rhizolith mineralogy†	Province
	Cgv (1·02–1·20)	Grey (5/N) massive silty claystone. Large (≈ 10 cm); horizontal, red (5R 4/8) Fe- and Mn-oxide nodules that coalesce to form a partially indurated polygonal network in plan view (Fig. 5B). Non-calcareous.	Haematite (60%)	K, I (43%)	
C: Inceptisol Markley Fm.	Ag (0–0·28)	Olive grey (5Y 5/2) mudstone with fine granular structure. Abundant fine- to medium-scale, subspherical white (5Y 2·5/1) mottles; fine-scale Fe-oxide nodules. Non-calcareous.	Variable horizon development from poor to moderate. Ped structure varies from moderately to well-developed, and medium to coarse angular and wedge-shaped.	Haematite (10%) K, I (22%)	Lower and upper coastal; piedmont
	Bv (0·28–0·49)	Olive (5Y 4/4) mudstone with medium angular blocky structure. Fine- to medium-scale, dusky red (10R 4/4) haematite nodules coalesced to form a semi-indurated layer. Non-calcareous.		Haematite (25%) K, I (25%)	
	BCssg(0·49–1·31)	Dark olive grey (5Y 3/2) mudstone with wedge- to lenticular-shaped structural aggregates defined by slickensides. Common, medium- to coarse-scale yellow (10YR 7/6) to dusky red (10R 4/4) mottles. Non-calcareous.		– K, I (32%)	
	Cg (131-cover)	Dark olive grey massive to poorly laminated mudstone. Abundant medium-scale, spherical to laminar light reddish brown (5YR 6/4) mottles. Non-calcareous.		– K, I (29%)	

Table 1. (Continued).

Pedotype and stratigraphic occurrence	Horizon depth (m)*	Macromorphology	Type profile variation	Nodule and rhizolith mineralogy†	Clay mineralogy‡ ≤ 2 µm	Province
D: Vertisol Markley Fm.	ABw (0–0.15)	Pale red (5R 4/2) mudstone with medium rhombohedral structure; superimposed fine granular structure. Abundant fine- to medium-scale, light green-grey (8/5 BG) mottles. Clastic-filled dykes extend through horizon. Non-calcareous.	Haematite nodules may be lacking.	–	I, I/S, K (28%)	Upper coastal; piedmont
	Bgc (0.15–0.35)	Grey (6/N) mudstone with medium rhombohedral structure. Common medium-scale dusky red (10R 3/4) mottles and haematite nodules. Clastic dykes extend to bottom of horizon. Non-calcareous.		Haematite (10%)	I/S, I, K (33%)	
	Bss (0.35–0.75)	Reddish-brown (5YR 5/4) mudstone with wedge-shaped structural aggregates defined by slickensides. Common medium- to coarse-scale, light green-grey mottles (8/5 BG). Non-calcareous.		–	I, K (39%)	
	2C (0.75–1.07)	Light green-grey (8/10Y) poorly laminated mudstone. Non-calcareous.		–	I, K (36%)	
E: Entisol Markley Fm. Archer City Fm. Nocona Fm. Petrolia Fm. Waggoner Ranch Fm.	AC (0–0.91)	Dusky red (7.5R 3/2) massive to weakly bedded fine-grained muddy sandstone. Branching networks of fine-scale mottling and thick, vertical, tubular light grey (7/N) mottles. Non-calcareous.	Variable development of redoximorphic features including gleyed matrix, mottling and/or Fe-oxide nodules. Weak development of slickensides	–	K, I (31%)	Lower and upper coastal; piedmont

Table 1. (Continued).

Pedotype and stratigraphic occurrence	Horizon depth (m)*	Macromorphology	Type profile variation	Nodule and rhizolith mineralogy†	≤ 2 µm Clay mineralogy‡	Province
	Cc (0.91–1.40)	Weak red (5R 3/3) fine-grained muddy sandstone. Common, fine to coarse dusky red (7.5R 4/3) mottles and haematite nodules. Non-calcareous.	Haematite (5%)	K, I (29%)		
F: Alfisol Archer City Fm. Nocona Fm. Petrolia Fm. Waggoner Ranch Fm.	AB (0–0.08) Bt1 (0.08–0.23)	Dark yellow-brown (10YR 6/4) mudstone with subangular blocky structure. Few fine- to medium-scale, pale red (10YR 4/4) vermicular mottles. Non-calcareous. Pale red (10R 6/4) silty claystone with medium angular blocky structure. Common, medium- to coarse-scale very pale red (10R4/3) vertical tubular mottles. Abundant clay skins on ped surfaces. Non-calcareous. Very pale red (10YR 4/3) silty claystone with medium angular blocky structure. Common, medium- to coarse-scale reddish-yellow (7.5YR 6/6) vertical tubular mottles. Abundant clay skins on ped surfaces. Non-calcareous.	Variable thickness profiles (0.7 m to 2 m). In some type F palaeosols, carbonate is not present or occurs overlying or superimposed on clay-rich horizons (i.e. polygenetic soils).	– –	S, K (30%) S, K (56%)	Lower and upper coastal; piedmont
	Bt2 (0.23–0.53)			–	S, K (61%)	
	Btk (0.53–0.79)	Brown-yellow (10YR 5/3) silty claystone with medium angular blocky structure. Abundant clay skins on ped surfaces. Abundant stage II carbonate nodules.		Calcite (10%)	S, K, I/S (57%)	
	BC _{ss} (0.79–1.06)	Red (7.5R 4/6) mudstone with wedge-shaped structural aggregates defined by slickensides. Very weakly calcareous.		–	S, I/S, K (33%)	

Table 1. (Continued).

Pedotype and stratigraphic occurrence	Horizon depth (m)*	Macromorphology	Type profile variation	Nodule and rhizolith mineralogy†	≤ 2 µm Clay mineralogy‡	Province
	C (1.06–1.76)	Dark yellowish-brown (10YR 4/4), massive to weakly laminated mudstone. Non-calcareous.	–	I/S, S, K (33%)		
G: Vertisol Archer City Fm. Nocona Fm. Petrolia Fm. Waggoner Ranch Fm.	ABk (0–0.27)	Reddish-brown (2.5YR 4/4) mudstone with medium prismatic structure; superimposed medium angular blocky structure. Abundant stage II carbonate nodules (Fig. 8G).	Carbonate development lacking in some type G palaeosols.	Calcite (10%)	S, K (33%)	Lower and upper coastal; piedmont
	Bkss1 (0.27–0.57)	Reddish-brown (2.5YR 4/4) mudstone with wedge-shaped structural aggregates defined by slickensides. Trace reddish-brown (5YR 5/3) spherical mottles. Clastic dykes extend through horizon. Abundant stage II carbonate nodules.		Calcite (15%)	S, K (30%)	
	Bkss2 (0.57–0.98)	Reddish-brown (2.5YR 4/3) mudstone with wedge-shaped structural aggregates defined by slickensides. Clastic dykes extend through horizon. Abundant stage II carbonate nodules.		Calcite (10%)	S, K (30%)	
	BCss (0.98–1.40)	Reddish-brown (2.5YR 4/3) mudstone with wedge-shaped structural aggregates defined by slickensides. Few to abundant medium-scale, reddish-brown (2.5YR 5/3) mottles. Clastic dykes extend to base. Very weakly calcareous.		–	S, I/S, K (27%)	
	C (1.40–2.11)	Dusky red (2.5YR 3/2) poorly laminated mudstone. Few medium grey (6/5BG) spherical mottles. Very weakly calcareous.		–	S, I/S (23%)	

Table 1. (Continued).

Pedotype and stratigraphic occurrence	Horizon depth (m)*	Macromorphology	Type profile variation	Nodule and rhizolith mineralogy†	≤ 2 µm Clay mineralogy‡	Province
H: Aridisol Archer City Fm. Nocona Fm.	Bkm (0–0.22)	Reddish-grey (2.5YR 6/1) mudstone; stage III carbonates.	Degree of carbonate development varies; morphologies can be nodular to tubiform (e.g. Fig. 8E). Matrix structure varies between prismatic, angular blocky and subangular blocky.	Calcite (95%)	I, K	Lower and upper coastal; piedmont
Petrolia Fm. Waggoner Ranch Fm.	Bk1 (0.22–0.39) Bk2 (0.39–0.58)	Yellow (10YR 7/6) mudstone with medium subangular blocky structure. Abundant stage II carbonate nodules. Pale red (5R 4/3) mudstone with medium to coarse angular blocky structure. Abundant stage II carbonate nodules.	Some type H palaeosols in Waggoner Ranch Fm. have slickenside planes filled by calcium carbonate at depth.	Calcite (35%) Calcite (10%)	I, K (22%) I, I/S, K (25%)	
	2Bss (0.58–0.76)	Pale red (10R 5/3) sandy mudstone with wedge-shaped aggregate structure defined by weakly developed slickensides. Calcareous.		–	I, I/S, K (22%)	
	3Cs (0.76–1.30)	Reddish-grey (10R 5/1) sandy mudstone with wedge-shaped aggregate structure defined by weakly developed slickensides. Few fine- to medium-scale grey-brown (10YR 5/2) subspherical mottles. Very weakly calcareous.		–	I, I/S, K (25%)	
	4C (1.30–1.60)	Grey-brown (10YR 5/2) massive to weakly bedded fine-grained sandstone. Moderate development of fine- to medium-scale yellow-brown (10YR 5/6) vermicular mottles. Very weakly calcareous.		–	–	

* Down-profile depth from the interpreted palaeosurface.

† Percentage of the matrix represented by Fe-oxide, jarosite or carbonate nodules and rhizoliths.

‡ Clay mineralogy presented in relative order of abundance in <2 µm size fraction; numbers in parentheses are percentage of matrix represented by this size fraction: K = kaolinite, I = illite, I/S = interlayered illite-smectite, S = smectite. Clays referred to in this study as illite are formally classified as mica-like minerals or sericite.

Key to Symbols		Horizons	
	Clastic dykes	O - horizons dominated by fossil organic matter.	
	Trough cross-bedding	A - Mineral surface horizon: obliteration of sedimentary structure; high organic content and abundant fine rhizoliths common.	
	Planar crossbedding	B - Mineral subsurface horizon: obliteration of sedimentary structures; represents zone of accumulation and may contain illuvial concentration of clay, iron, aluminum, carbonate, gypsum, and silica.	
	Planar lamination	C - Mineral subsurface horizon: minimally affected by pedogenic processes; lacks properties of O, A, or B horizons.	
	Ripple cross lamination	Horizon Descriptors	Lithologic Descriptors
	Wavy laminations		
	Limestone	c - concretions	o - organic layer
	Palaeofloral deposits	g - strong gleying	c - clay
	Rhizoliths	i - slightly decomposed organic matter	s - silt
	Fe-(Mn) oxide nodules	j - jarosite accumulation	f - fine sand
	Fe-(Mn) oxide-rich horizon (plinthite)	k - carbonate accumulation	m - medium sand
	carbonate rhizoliths	m - cementation or induration	C - coarse sand
	Carbonate nodules	ss - slickensides	ca - limestone
	Calcified slick planes	t - clay accumulation	g - gypsum
	Laminar calcrite	v - plinthite(indurated Fe-oxide layers)	
	Pedogenic Slickensides	w - develop. of soil colour or structure but little if any illuvial accumulation	
	Angular blocky structure	Numerical Descriptors	
	Conglomerate	Numbers are used to distinguish between horizons with the same letter descriptors from individual profiles (e.g., Bkss1 and Bkss2). Numerals placed before letter descriptors are used to differentiate horizons from the same profile that formed in different lithologies (e.g., 2Bss, 3Css).	
	Lime Pebble Conglomerate		
	coaly shales		
	Columnar structure		

Fig. 3. Key of symbols and horizon nomenclature used in Figs 4, 7 and 9–13.

interpreted as being the product of similar soil-forming environments in which local and regional processes combined to produce a distinctive profile. Pedotypes are thus analogous to a soil series in a modern landscape (Retallack, 1990; Bestland *et al.*, 1997).

In the following section, the pedotypes are described based, in part, on individual measured profiles judged to be most representative of all palaeosols assigned to a given group. Major variations in morphology or composition from the type profile are discussed and summarized in Table 1. The pedotypes are related to the USDA soil taxonomy classification (Soil Survey Staff, 1975, 1998), the spatial and stratigraphic distribution of the associated palaeosols delineated and the palaeoenvironmental implications assessed.

Type A palaeosols

Description

The type profile of pedotype A is composed of three non-calcareous layers that define a thin profile (0.4 m; Figs 3 and 4A, Table 1). The uppermost dark grey to black, massive layer is organic rich and dominates the profile (Fig. 5A). The underlying light grey claystone layer exhibits angular structure, is composed of quartz silt and low cation-exchangeable clays (kaolinite and subordinate amounts of illite; Table 1) and lacks labile minerals (biotite, muscovite, feldspars) present in the unaltered parent material. The basal grey claystone layer contains a small amount of labile minerals and lacks clear pedogenic features. Redoximorphic features (e.g. Vepraskas, 1994) are abundant in type A

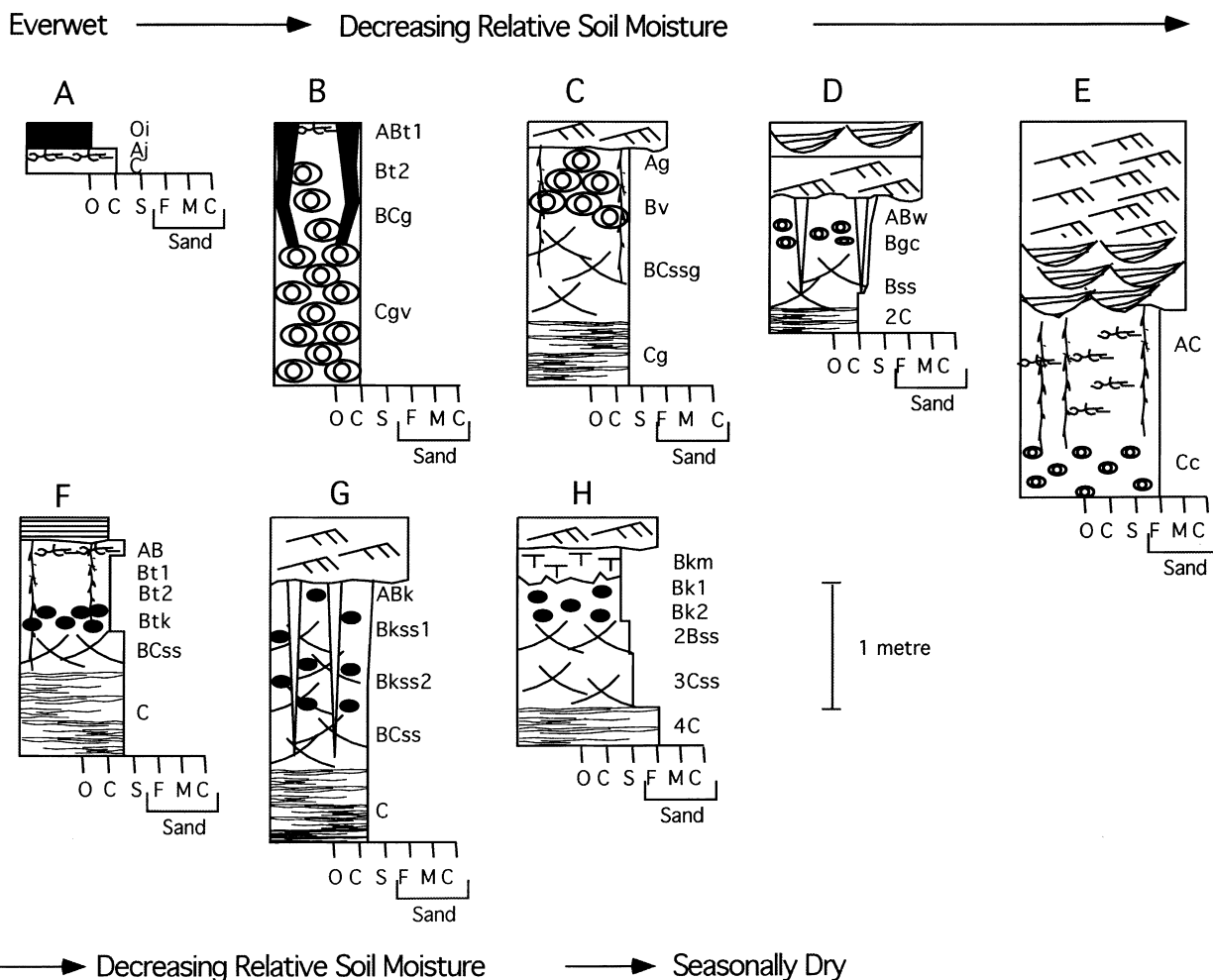


Fig. 4. Measured sections of palaeosol profiles representative of each of the eight pedotypes. (A) Type A palaeosol from the Late Pennsylvanian Markley Fm., site 1 (Fig. 1). (B) Type B palaeosol, Markley Fm., site 1. (C) Type C palaeosol, Markley Fm., site 4. (D) Type D palaeosol, Markley Fm., site 5. (E) Type E palaeosol, Markley Fm., site 6. (F) Type F palaeosol from the Archer City Fm., site 11. (G) Type G palaeosol from the Waggoner Ranch Fm., site 26. (H) Type H palaeosol, Waggoner Ranch Fm., site 28.

palaeosols and include overall low chroma matrix colours (gleying), tabular networks of downward-bifurcating rhizoliths and medium to coarse yellow mottling. Rhizoliths in the type palaeosol are replaced by jarosite.

Type A palaeosols are developed within silty mudstones of the floodplain facies; all type A palaeosols are laterally discontinuous over tens to hundreds of metres (e.g. see sections 1 and 2 in Fig. 6). These palaeosols occur as thin (averaging <0.5 m) composite profiles (*sensu* Marriott & Wright, 1993; Kraus, 1999) with common thin clastic partings. They are stratigraphically restricted to sites 1–3 in the lower half of the Upper Pennsylvanian Markley Formation (below ss11 in Fig. 2).

Interpretation and classification

Laterally discontinuous, organic matter-rich layers in type A palaeosols are interpreted to be surficial accumulations (O horizons) that formed by *in situ* accumulation of plant material (Figs 4A and 5A). Angular blocky structure in the underlying claystone layer is interpreted as being ped structure that formed by differential shearing of plastic materials (clays) in the profile. The gleyed matrix, lack of weatherable labile minerals, low organic content and abundance of kaolinite in the ≤2 μm size fraction suggest that the claystones directly underlying O horizons formed as eluvial A horizons in response to intense hydrolysis or acidolysis in poorly drained profiles (Fig. 4A; cf. van Breeman & Harmsen, 1975).

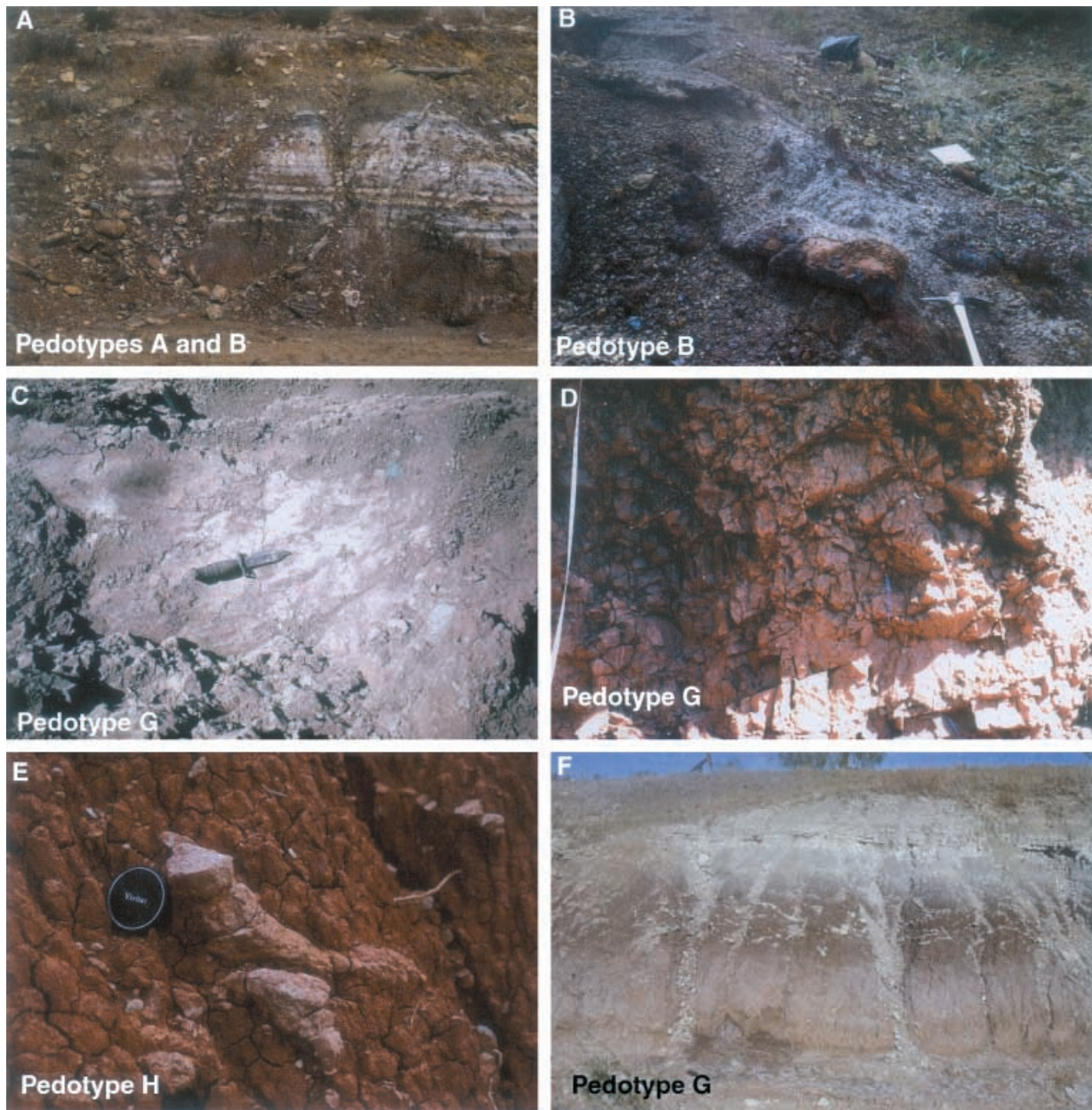


Fig. 5. Macromorphologies of Permo-Pennsylvanian palaeosols. (A) Couplets of dark–light banding are type A palaeosols; dark layers are O horizons, light layers are A horizons. Approximately 1.7 m thick dark horizon at base of outcrop is a type B palaeosol. Palaeosols are from the Upper Pennsylvanian Markley Fm., site 2. (B) Haematite redox concentrations, oriented into a polygonal pattern (1.5 m across), in the Cgv horizon of a type B palaeosol, Markley Fm., site 1. (C) Slickensides in a type G palaeosol, Lower Permian Nocona Fm., locality 15. Knife (0.25 m long) for scale; blade points in the direction of mineral orientation along the slickensurface. (D) Type G palaeosol showing pedogenic slickensides in cross-section, Lower Permian Waggoner Ranch Fm., site 26. White ‘blebs’ are pedogenic carbonate nodules. Field of view is 1.5 m. (E) Calcareous rhizoliths from a type H palaeosol, Waggoner Ranch Fm., site 31. 35 mm lens cap for scale. (F) Type G palaeosol, upper Waggoner Ranch Fm., site 31. Overlying light-coloured beds are marine calcareous silts and limestones of the Maybelle Limestone.

Type A palaeosols are interpreted as being histosols (Soil Survey Staff, 1998) given the relative thickness and concentration of organic matter in the O horizons of the palaeosol profiles (Fig. 4A). Modern histosols form in low-lying, waterlogged regions characterized by always wet

conditions and anoxic pore waters that promote *in situ* accumulation of organic matter. The predominance of gley matrix colours and low chroma mottles and root traces in type A palaeosols, as well as the paucity of discrete Fe-oxide nodules, supports prolonged saturation of these

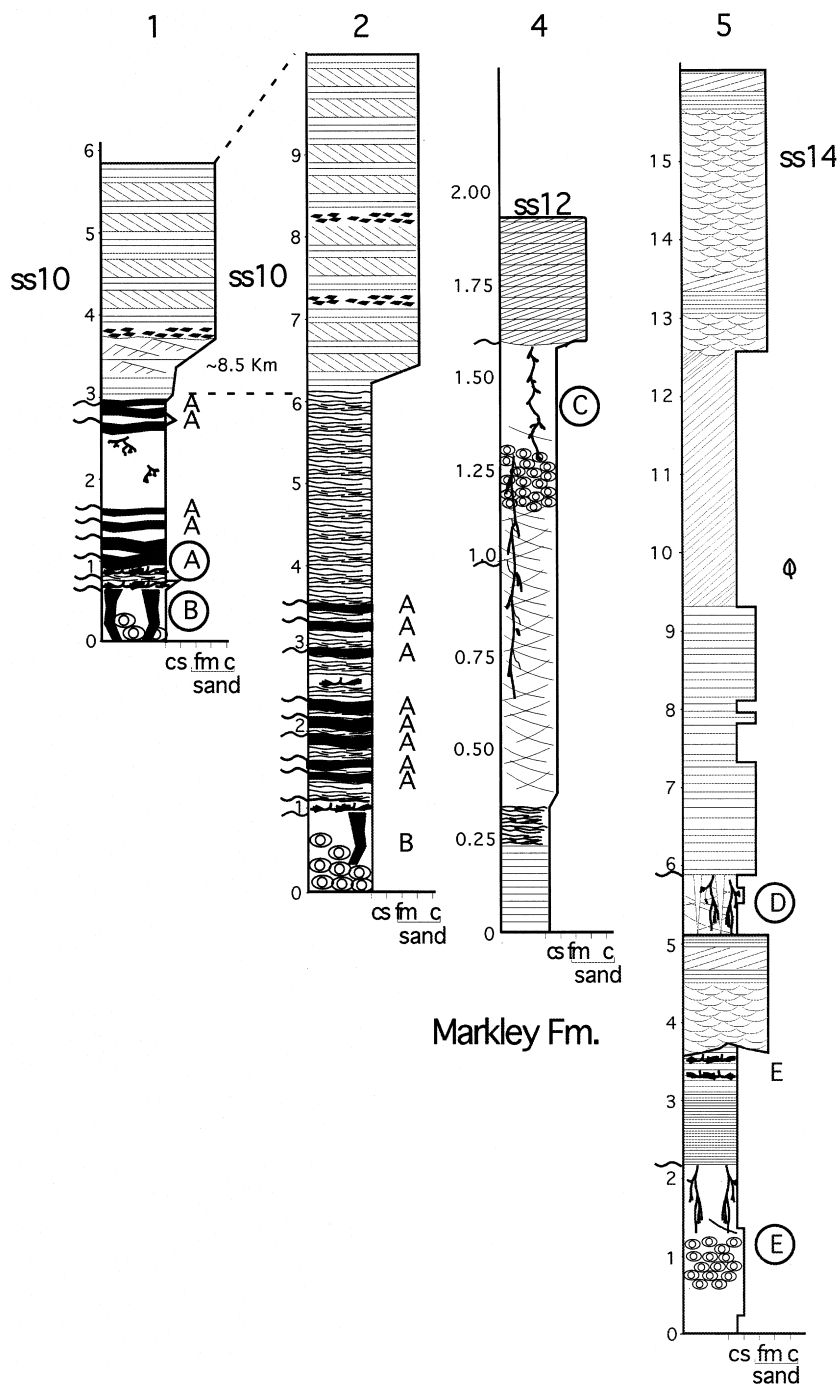


Fig. 6. Palaeosol-bearing sections of Upper Pennsylvanian Markley Formation. Palaeosol tops are delineated by wavy 'lines' to the left of each measured section. Capital letters refer to palaeosols of a given pedotype; circles delineate pedotype profiles discussed in the text. Sections 1 and 2 are from two outcrops separated by 8.5 km; correlation between outcrops based on sandstone set 10 (ss10) in the middle of the Markley Fm. Measured section 4 underlies sandstone set 12 (ss12) in the upper portion of the Markley Fm. Measured section 5 underlies ss14 from the uppermost Markley Fm., proximal to the Pennsylvanian–Permian boundary. See Fig. 2 for stratigraphic position of sandstone sets.

profiles (Simonson & Boersma, 1972; Wilding *et al.*, 1983; Schwertmann, 1985). The shallow and tabular distribution of jarosite-replaced roots in fossil A horizons further reflects the poorly drained palaeosol conditions (cf. Retallack, 1988, 1990). Jarosite, however, may represent post-pedogenic oxidation of Fe-sulphides despite its neomorphic replacement of roots (cf. Kraus, 1998).

Late Pennsylvanian type A palaeosols are interpreted as having formed in poorly drained, shallow depressions on the regionally extensive coastal plain given their morphological characteristics and laterally discontinuous nature. The predominance of stacked, thin, composite profiles (Fig. 6) reflects slow, episodic sediment accumulation in geomorphic lows on the latest Pennsylvanian coastal plain of western equatorial Pangea.

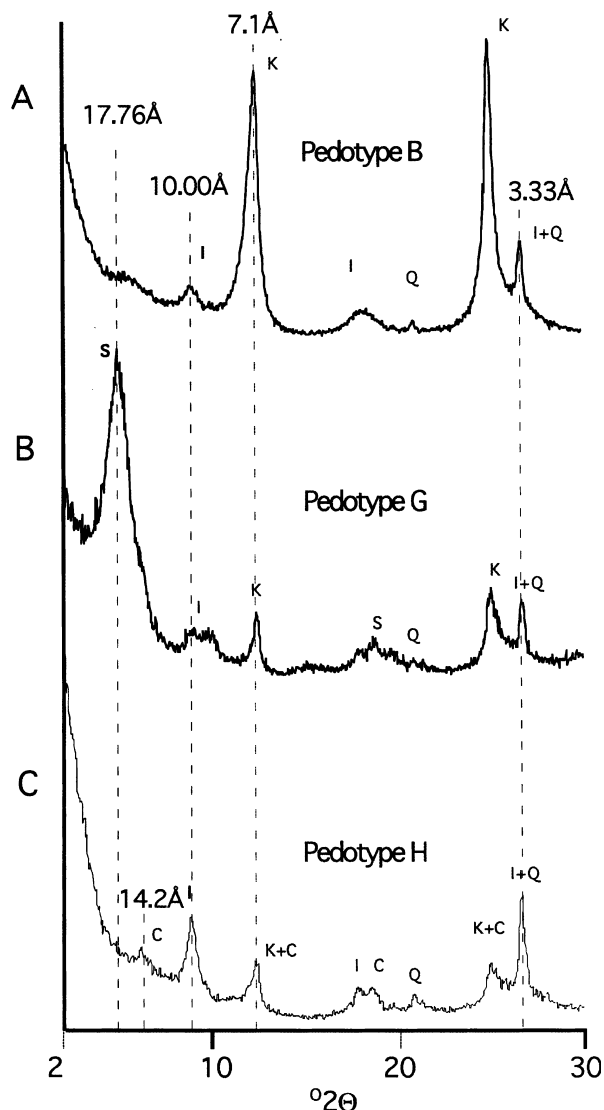


Fig. 7. XRD patterns of clay minerals from the $\leq 2 \mu\text{m}$ size fraction in select type palaeosols. Clay mineralogy of: (A) a Bt horizon; type B palaeosol, Upper Pennsylvanian Markley Fm.; (B) Bt horizon, type G palaeosol, Lower Permian (lower Leonardian) Petrolia Fm.; (C) Bk horizon, type H palaeosol, Lower Permian (mid-Leonardian) Waggoner Ranch Fm. K = kaolinite; I = illite; S = smectite; C = hydroxy-interlayered minerals; Q = quartz.

Type B palaeosols

Description

The type profile of pedotype B (Figs 4B and 6) is composed of four distinct units: (1 and 2) two upper, red claystones that exhibit fine angular to subangular blocky structure and oriented clay and Fe-oxide coatings along matrix aggregates and lining channel voids; (3) an underlying, mottled red/grey silty claystone that exhibits subangular blocky structure; and (4) a basal,

massive grey silty claystone (Fig. 4B; Table 1). Redoximorphic features are present throughout the profile as redox depletions (i.e. low chroma mottles and matrix colours) and as redox concentrations (i.e. Fe- and, less commonly, Mn-oxide coatings on matrix aggregates and Fe-oxide nodules). Oblate Fe-oxide nodules, ranging from 0.05 to 0.2 m in length, are laterally oriented and form a partially indurated horizon at the base of the type profile (Fig. 5B). Type B palaeosols with less well-differentiated horizons commonly lack thick accumulations of Fe-oxides.

Kaolinite and trace amounts of illite dominate the $\leq 2 \mu\text{m}$ size fraction of all claystones; labile minerals are generally lacking (Fig. 7A). The abundance of the clay-dominated, $\leq 2 \mu\text{m}$ size fraction decreases downprofile (e.g. from 78% to 43%; Table 1).

Type B palaeosols occur primarily as thin to moderately thick ($< 1.5 \text{ m}$), strongly developed profiles within mudstones of the floodplain facies (Figs 5A and 6). Type B palaeosols are stratigraphically associated with type A palaeosols. Type B palaeosols are primarily developed upon mudstones and are stratigraphically limited to the lower half of the Upper Pennsylvanian Markley Formation (below ss11 in Fig. 2).

Interpretation and classification

Redoximorphic colouration and the abundance of moderate to large Fe-oxide nodules in the lower portion of profiles (BCg and Cgv horizons in Fig. 4B) indicate that type B palaeosols were waterlogged for prolonged periods (i.e. hydromorphic soils), given that the degree of chemical weathering of parent material and the size and abundance of Fe-oxide nodules commonly increase with increased duration of waterlogging (Simonson & Boersma, 1972; Sobocki & Wilding, 1983; Retallack, 1990). However, the predominance of kaolinite in the clay fraction indicates that these hydromorphic soils were characterized by episodic or seasonal changes in soil moisture conditions (Wilding *et al.*, 1983; Schwertmann, 1985; Dixon & Skinner, 1992).

Clay-rich horizons in type B palaeosols are interpreted as being zones of clay accumulation or argillic horizons (ABt1 and Bt2 in Fig. 4B) that formed by downward translocation of clay minerals (i.e. illuviation). Concentration of clay minerals, in particular kaolinite, in the inferred Bt horizon and the presence of continuous, oriented clay coatings (argillans of Brewer, 1976) on peds and lining channel voids suggest extensive pedogenic kaolinite formation. The presence of Fe-oxide (and less commonly Mn-oxide;

ferri-mangans of Brewer, 1976) lining peds and voids, in addition to the downprofile increase in Fe-oxide nodules, records downward translocation of Fe and Mn in addition to clay minerals. Translocation and mineral accumulation also indicate that type B hydromorphic palaeosols underwent periods of free drainage (Birkeland, 1999).

The haematite- and goethite-cemented layers at the base of type B palaeosols are analogous to modern plinthites that form in soil horizons characterized by a seasonally fluctuating water table (Duchaufour, 1982; Soil Survey Staff, 1998). The thickness of the palaeoplinthite horizon (≈ 1 m) and its depth below the palaeosol surface suggest that the local palaeowater table probably fluctuated within 1–2 m of the land surface (cf. Duchaufour, 1982).

Type B palaeosols are interpreted as ultisols based on morphological evidence for argillic horizons, prolonged saturation and extensive hydrolysis interrupted by episodes of free drainage. Modern ultisols form in warm, humid environments (e.g. modern tropical rainforests) characterized by high rates of chemical weathering. These soils minimally require periodic drainage in order to form argillic horizons through illuviation (Retallack & German-Heins, 1994; Gill & Yemane, 1996). Although Late Pennsylvanian ultisols formed penecontemporaneously with type A palaeosols, ultisols are interpreted as having formed on stable landscapes such as interchannel highs that may have developed during minor episodes of fluvial downcutting. This interpretation is based on evidence for their strong pedogenic development and for their having been at least episodically well-drained in the upper argillic horizons of the profile (cf. Markewich & Pavich, 1991; Bestland *et al.*, 1997), and on the inferred low sedimentation rates recorded by their thin, composite profiles (cf. Marriott & Wright, 1993).

Type C palaeosols

Description

The type profile of pedotype C consists of four poorly to moderately developed horizons (Table 1) that exhibit fine to medium angular blocky structure. Larger scale wedge- to lenticular-shaped structural units are defined by randomly oriented slickensides that overprint the finer scale angular blocky structure in the lower mudstone (BC_{ssg} in Fig. 4C). Although all type C palaeosols exhibit some structure that is indicative of pedogenic development, most profiles only have weak horizonation. Abundant redoximorphic concentrations (yellow

to reddish-brown mottles and Fe-oxide nodules) and reductions (gleyed matrix colours) occur throughout type C palaeosols (Fig. 8A). A semi-indurated layer of coalesced submillimetre-sized haematite nodules (Fig. 8D) occurs near (28–49 cm depth) the interpreted palaeosurface of the type profile (Fig. 4C); analogous Fe-oxide layers are lacking in some type C palaeosols. The $< 2 \mu\text{m}$ size fraction contains a moderate amount of clay minerals (22–32%) that are dominated by illite and subordinate amounts of kaolinite and hydroxy-interlayered mineral (HIM) clays.

Type C palaeosols occur as thick compound and composite profiles (Fig. 6) developed in intercalated thinly bedded mudstones, siltstones and fine-grained sandstones. They are stratigraphically restricted to overbank mudstone deposits associated with channel and crevasse-splay sandstone deposits in the Upper Pennsylvanian Markley Formation above fluvio-genic cycle ss11 (sites 4 and 5; Figs 2 and 6).

Interpretation and classification

The laterally continuous, semi-indurated Fe-oxide layer in the upper part of the type profile is interpreted as being a palaeoplinthite (B_v horizon in Fig. 4C). The development of a plinthite proximal to the palaeosol surface records a shallow, fluctuating palaeogroundwater table (Table 1; cf. Duchaufour, 1982). Further evidence for fluctuating soil moisture conditions is the occurrence of large-scale wedge- to lenticular-shaped peds defined by slickensides in basal mudstones. Pedogenic slickensides form in clay-rich modern soils as a result of soil mass movement and structural modification driven by wetting and drying cycles (Dudal & Eswaran, 1988; Wilding & Tessier, 1988). Limited development of large-scale peds and slickensides in type C palaeosols, however, suggests modest fluctuations in soil moisture content in the lower portions of the profile and/or profile immaturity (Brewer, 1976; Jim, 1990), given that these features form rapidly in soils characterized by repeated wetting and drying (Yaalon & Kalmar, 1978; Birkeland, 1999).

Type C palaeosols are classified as inceptisols given their moderate development of ped structure and horizonation. These probably immature profiles formed in floodplain deposits proximal to fluvial channels, as evidenced by their close lateral and stratigraphic proximity to channel-filling and crevasse-splay sandstones; their compound and cumulate profiles record steady, and sometimes rapid, sedimentation in these environments (cf. Marriott & Wright, 1993; Kraus, 1999).

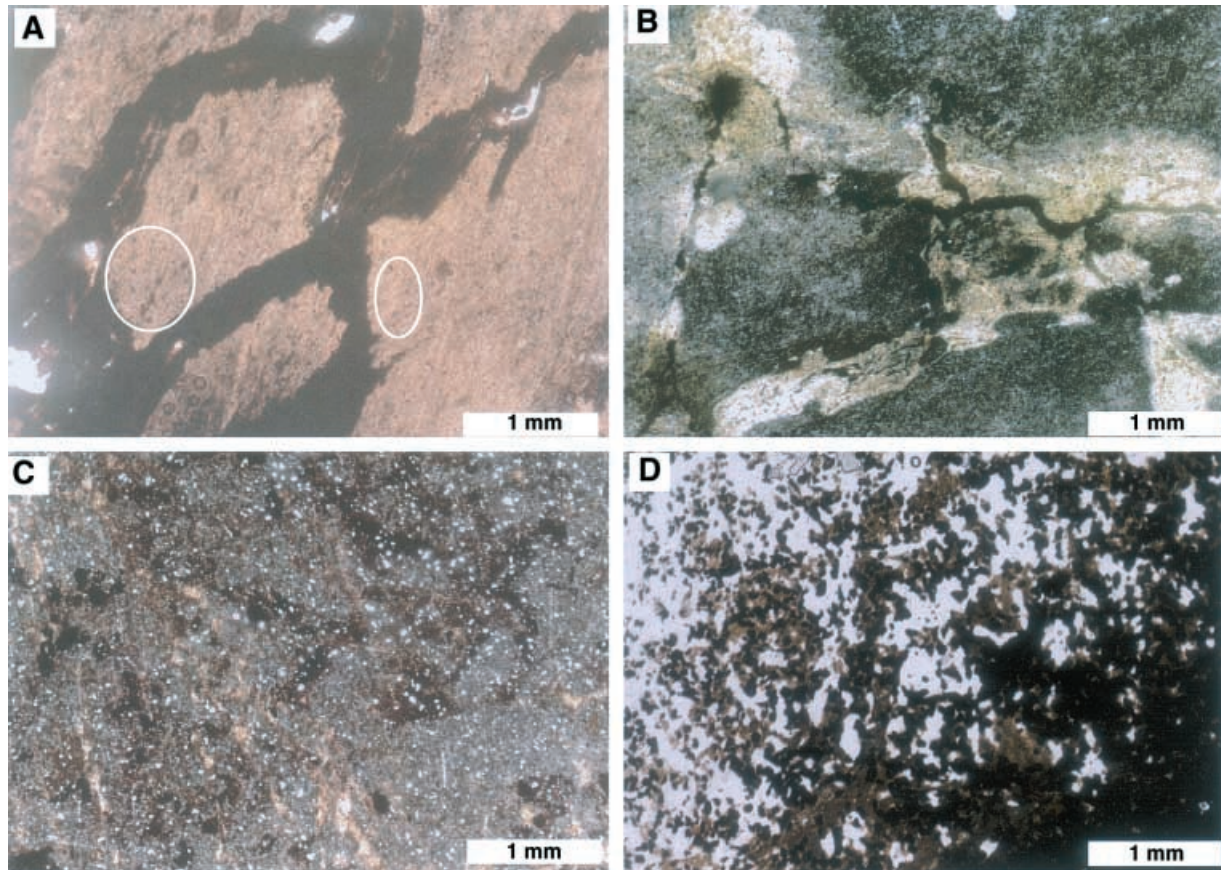


Fig. 8. Photomicrographs of redoximorphic features in Upper Pennsylvanian palaeosols. (A) Haematite nodules (e.g. dark spots in area marked by white ovoids) and ferrans (dark area) in a claystone (Bv horizon) with angular blocky structure; type C palaeosol. Scale bar = 1 mm. (B) Redoximorphic depletions (light grey) and concentrations (dark grey) in an AC horizon; type E palaeosol. Scale bar = 1 mm. (C) Redoximorphic depletions (light grey) and concentrations (black) of both diffuse and nodular haematite in a Cc horizon; type E palaeosol. Scale bar = 1 mm. (D) A plinthite horizon altered to an ironstone; the ironstone is composed predominantly of haematite nodules (black) and a minor amount of clay minerals; type C palaeosol. Scale bar = 1 mm.

Type D palaeosols

Description

The type profile of pedotype D is composed of four red to grey mudstone units that exhibit abundant redoximorphic features including small (≈ 10 mm) haematite nodules, manganese oxide coatings and low chroma soil matrix (or gley) colours (Fig. 4D; Table 1). The top two units exhibit medium-scale (50–200 mm long) rhombohedral structural aggregates; the uppermost claystone exhibits superimposed angular blocky structure defined by clay-lined microslickensides. Clay-rich mudstones in the lower half of the profile exhibit wedge-shaped structural aggregates defined by larger scale slickensides. Clay and Mn-oxides typically coat slickensides. Sand-filled V-shaped dykes (Figs 3D and 6) cross-cut the upper half of the type profile. The $< 2 \mu\text{m}$ size

fraction in the type profile is dominated by hydroxy-interlayered minerals and smectite and lesser amounts of kaolinite (Table 1).

Type D palaeosols are developed within mudstones of the sand- and gravel-rich channel-bar facies (Fig. 6) of the uppermost Upper Pennsylvanian Markley Formation (above ss13 in Fig. 2). Their distribution is limited to the eastern portion of the study area (sites 5 and 6 in Fig. 1).

Interpretation and classification

Well-developed, medium-scale rhombohedral- and wedge-shaped structure and associated pedogenic slickensides in type D palaeosols are analogous to ‘parallelepipeds’ in Holocene vertisols (Dudal & Eswaran, 1988). In modern soils, vertic features develop during mass movement and shearing in smectite-rich soils that become saturated during seasonal rainfall (Yaalon &

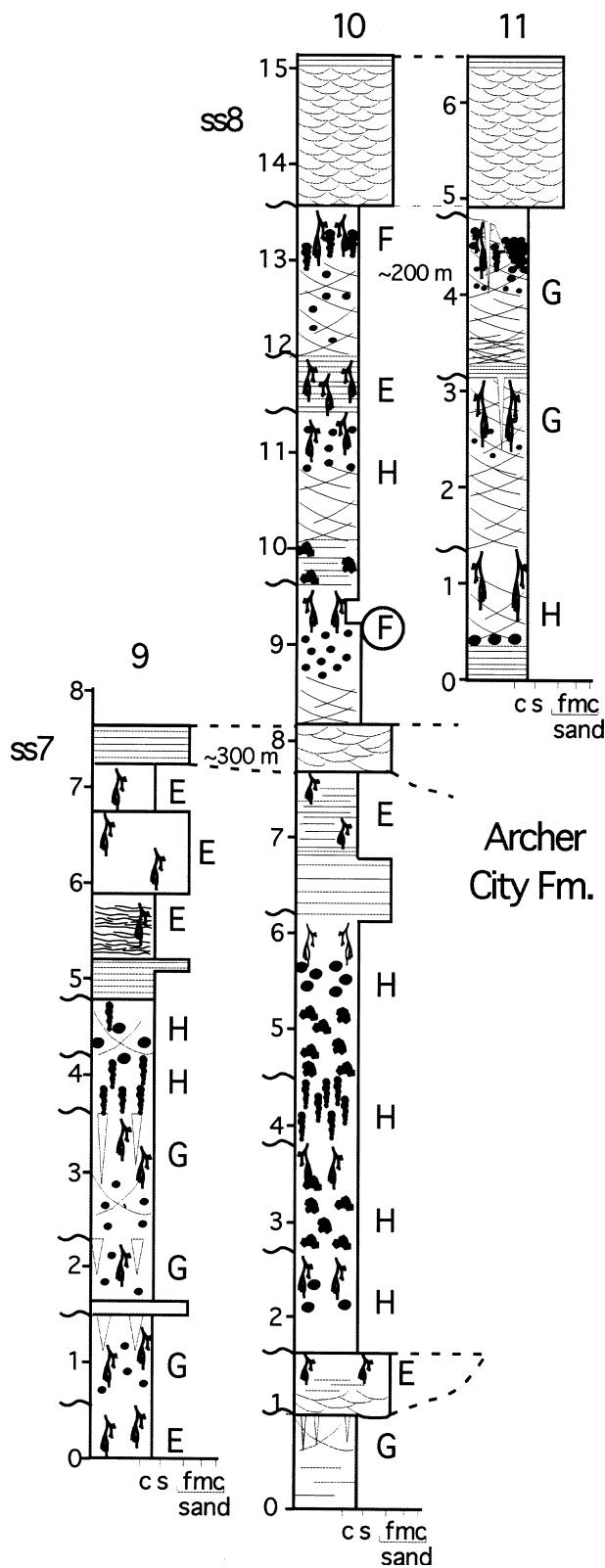


Fig. 9. Palaeosol-bearing sections of Lower Permian Archer City Formation. Palaeosol tops are delineated by the wavy lines to the left of each measured section. Capital letters refer to palaeosols of a given pedotype; circle delineates pedotype profile discussed in the text. Correlation of three sites (sites 9, 10 and 11 in Fig. 2) based on sandstone set 8 (ss8). Sites 9 and 10 are separated by 0.3 km, and sites 10 and 11 are separated by 0.2 km. See Fig. 3 for key to symbols.

stress cutans (Jim, 1990) due to differential wetting, and shrinking and swelling forces driven by repeated wetting and drying of the soil matrix. Decreasing soil moisture and shrinking of soil clays resulted in cracking of the soil matrix during drier intervals. The V-shaped dykes that cross-cut the upper portions of the profiles resulted from back-filling of these surficial cracks from sediment-laden water during subsequent flood events.

Type D palaeosols are classified as vertisols based on abundant and well-developed vertic features, their clay content (28–39%) with a significant percentage of smectite and the presence of deep V-shaped cracks developed within the upper horizons (Soil Survey Staff, 1998). Modern vertisols form in seasonally moist and typically tropical to warm-temperate climates, with four to eight dry months yearly (Dudal & Eswaran, 1988; Buol *et al.*, 1997). The relatively low kaolinite content and preservation of expandable 2:1 layer-lattice clays (smectite) in type D palaeosols coupled with the occurrence of clastic dykes indicate periods of drying that were sufficiently long to preserve expandable clay minerals and to allow for significant shrinkage of the clay-rich matrix (Duchaufour, 1982; Retallack, 1990). However, the presence of gley matrix colours and common to abundant redox depletions requires that periods of palaeosol moisture deficiency in type D palaeosols were temporally limited (Daniels *et al.*, 1971; Duchaufour, 1982; Buol *et al.*, 1997). Based on their stratigraphic association with overbank mudstones as well as the morphological and chemical characteristics of these palaeovertisols, they are interpreted as having formed in interfluvial muds on the Late Pennsylvanian upper coastal plain and piedmont.

Type E palaeosols

Description

The representative profile of pedotype E consists of two units that are very weakly developed in muddy fine-grained sandstone and are

Kalmar, 1978; Dudal & Eswaran, 1988; Wilding & Tessier, 1988). The thin clay coatings on superimposed angular blocky peds probably formed as

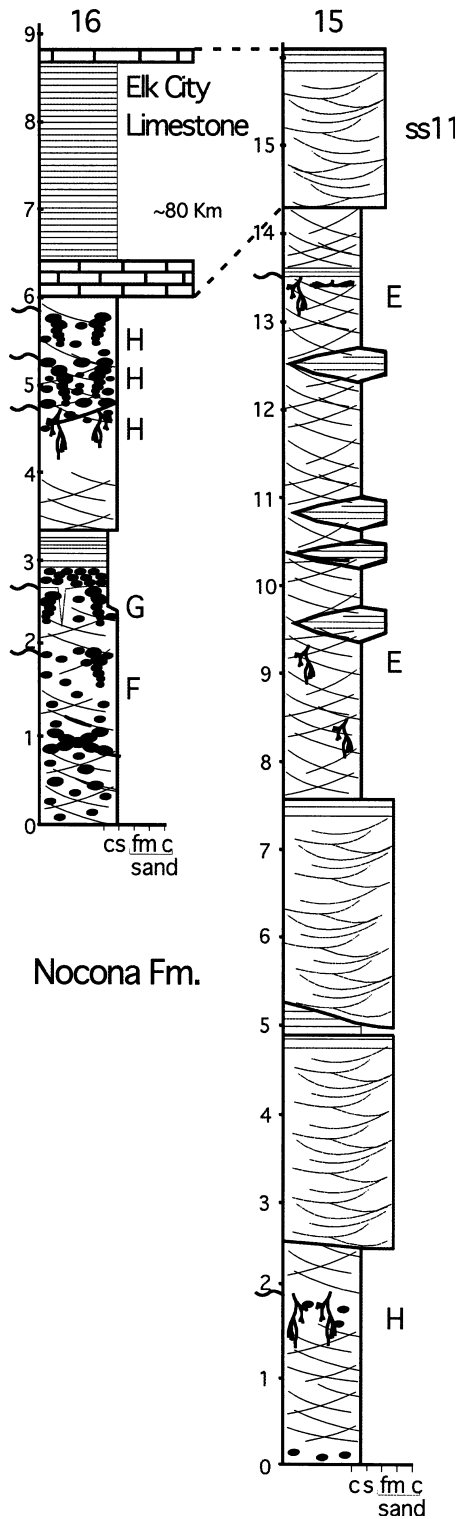


Fig. 10. Palaeosol-bearing sections of Lower Permian Nocona Formation. Palaeosol tops are delineated by the wavy lines to the left of each measured section. Capital letters refer to palaeosols of a given pedotype. Correlation of the siltstone- and claystone-dominated section from site 16 with the sandstone-dominated section at site 15 (80 km apart) based on contemporaneity of Elk City Limestone and ss11 defined by Hentz (1988). Key to symbols as in Fig. 3.

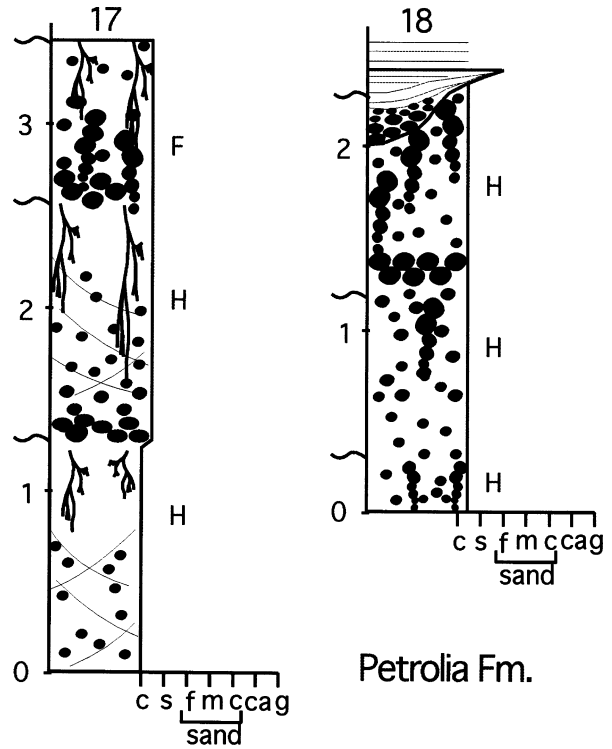


Fig. 11. Palaeosol-bearing sections of Lower Permian Petrolia Formation at sites 17 and 18. Palaeosol tops are delineated by the wavy lines to the left of each measured section. Capital letters refer to palaeosols of a given pedotype. Key to symbols as in Fig. 3.

distinguished by their colour and nature of the redoximorphic features (Fig. 4E; Table 1). The upper red unit exhibits a vertically oriented, branching network of light-grey, fine- (< 10 mm wide) to coarse-scale (10–25 mm wide) tubular

mottles (Figs 6 and 8B); superposition of different generations of mottles is observed. The lower pale red unit contains fine to coarse dark red mottles and haematite nodules (Fig. 8C). The < 2 µm size fraction in the profile is dominated by kaolinite and illite (Table 1). In addition, some type E palaeosols also exhibit weakly developed slickensides.

Type E palaeosols occur as thick (1–2 m) cumulate and compound and composite palaeosols throughout the Permo-Pennsylvanian terrestrial strata in the study area (sites 1–3, 5, 6, 9–11, 12–15, 19–22, 24, 25 and 29 in Fig. 1). They are developed within or stratigraphically adjacent to finely laminated to slightly bioturbated silty

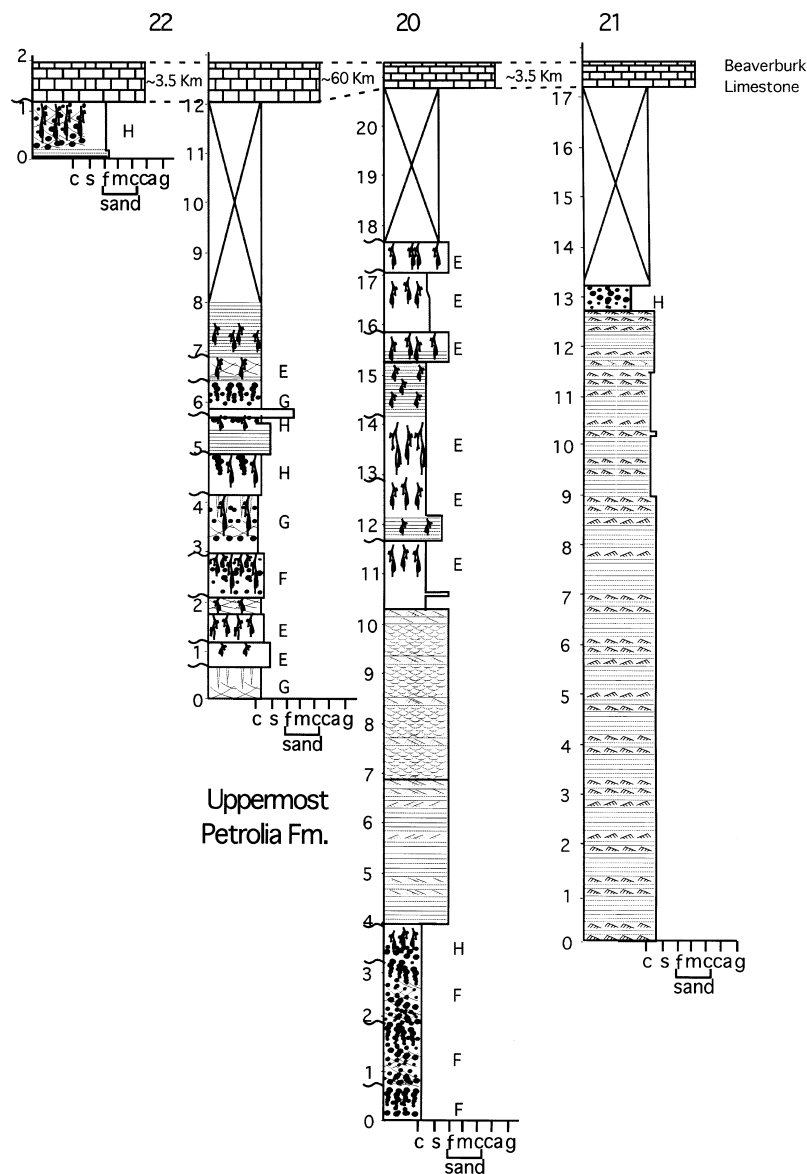


Fig. 12. Correlated transect (67 km long) of four palaeosol-bearing sections of the Lower Permian Petrolia Formation beneath the regionally traceable Beaverburk Limestone. The two sections (site 22) on the left are siltstone and claystone dominated, whereas sections from sites 20 and 21 contain abundant sandstones of the point-bar facies. Palaeosol tops are delineated by the wavy lines to the left of each measured section. Capital letters refer to palaeosols of a given pedotype. Key to symbols as in Fig. 3.

mudstones and siltstones and fine- to medium-grained sandstones of the channel bar and point bar facies (Figs 6, 9, 10, 12 and 13).

Interpretation and classification

Type E palaeosols are interpreted as entisols based on the very weak development of pedogenic structure and horization (Soil Survey Staff, 1998). Modern entisols exhibit little to no development of horization, and typically form upon unstable, wet landscapes (Buol *et al.*, 1997). Entisols record stunted horizon development resulting from prolonged saturation and/or limited periods of pedogenesis (tens to hundreds of years) caused by rapid sedimentation rates (Buol *et al.*, 1997). The occurrence of redoximorphic

depletions and concentrations in many type E palaeosols indicates a certain degree of hydro-morphy (waterlogging; cf. Simonson & Boersma, 1972; Fanning & Fanning, 1989).

In contrast, type E palaeosols that formed in sandy siltstones typically lack redoximorphic features. Given that many type E palaeosols commonly occur as weakly developed, compound or cumulate profiles in proximal positions to fluvial siltstones and sandstones and estuarine siltstones and mudstones (south-western portion of study area), they are interpreted as having formed on unstable landscapes proximal to fluvial channels (e.g. levees and crevasse splays) on the coastal plain and piedmont and wetlands of the lower coastal plain.

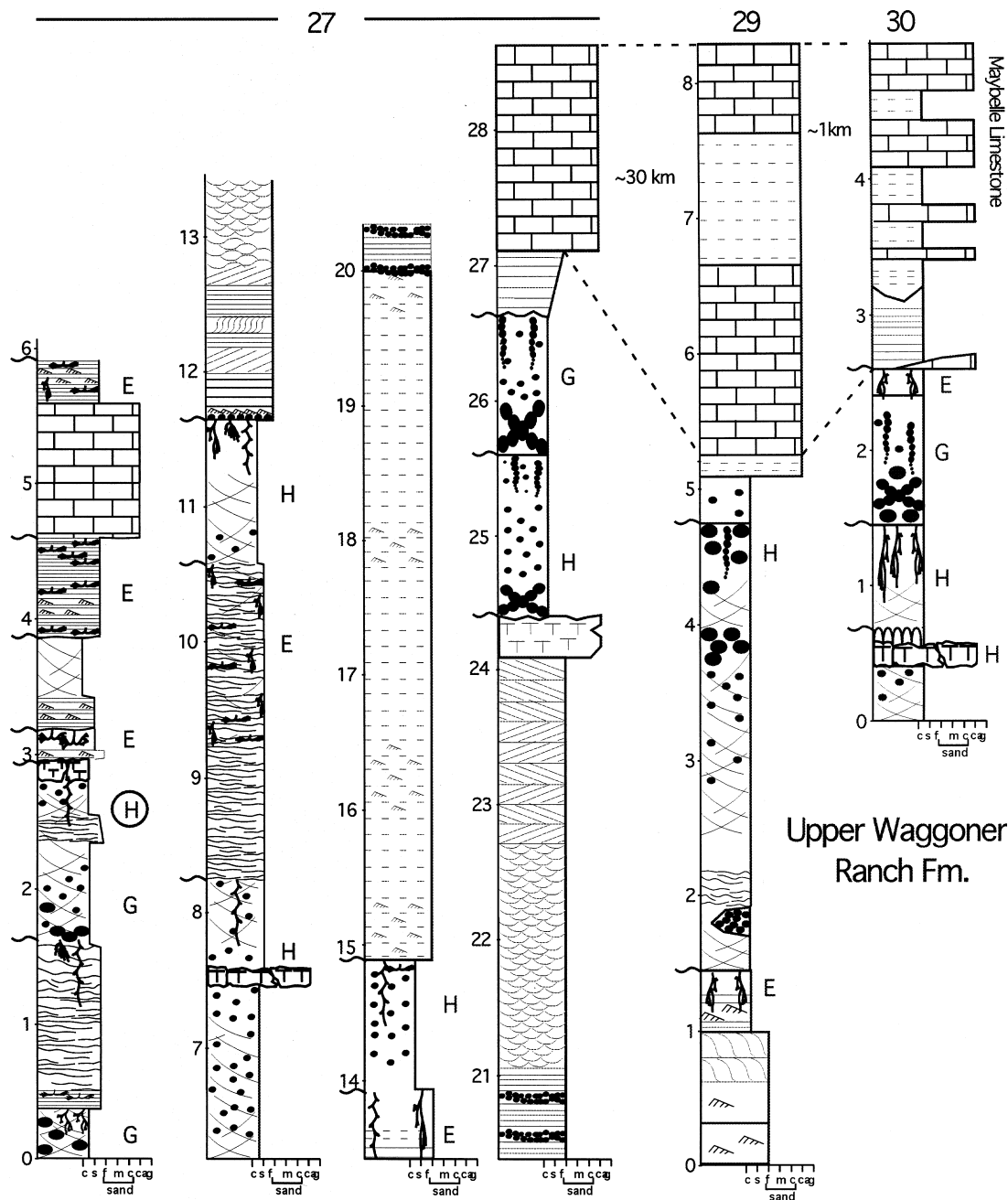


Fig. 13. Correlated transect (31 km long) of three palaeosol-bearing sections (from sites 27, 29 and 30) of the Lower Permian Waggoner Ranch Formation beneath the Maybelle Limestone. Palaeosol tops are delineated by the wavy lines to the left of each measured section. Capital letters refer to palaeosols of a given pedotype; circle delineates pedotype profile discussed in text. Key to symbols as in Fig. 3.

Type F palaeosols

Description

The type profile of pedotype F is composed of six well-developed horizons (Fig. 4F; Table 1) that are distinguished by their clay content, structure, mottling and mineral accumulations. The uppermost horizon is defined by a dark yellow-brown, non-calcareous mudstone with fine to medium

subangular blocky structure. Three significantly more clay-rich layers (56–61% clay vs. 30–33% in other units) underlie the uppermost mudstone. These are red to brown, silty claystones that exhibit fine to medium subangular blocky structure. Thick, continuous and oriented clay coatings (argillans) occur around detrital grains and line aggregates in all three claystones. The upper two claystone layers are non-calcareous, whereas

the lowermost claystone contains discrete, cm-scale stage II carbonate nodules (*sensu* Machette, 1985) and weakly developed calcareous rhizoliths (Figs 9–12) that exhibit pedogenic fabrics (cf. Deutz *et al.*, 2002). Faint tubiform red and reddish to yellow mottles in the mudstone and claystone layers define a pattern similar to branching root structures (cf. Retallack, 1988, 1990) and probably record deeply penetrating root systems. Smectite dominates the <2 µm size fraction of the claystone layers, with trace amounts of kaolinite and illite (Table 1). The lower two horizons in the type profiles are red and yellowish-brown mudstones (Table 1); the upper horizon exhibits wedge-shaped structural aggregates defined by randomly oriented slickensides, whereas the lower horizon preserves disturbed primary sedimentary laminations (Fig. 4).

Some variants of the type profile lack the horizon of stage II carbonate nodules. Moreover, some type F palaeosols contain carbonate-rich horizons that overlie or are superimposed on the clay-rich horizons with clay skins (cutans). These dominantly strongly developed palaeosols may occur as composite profiles and are found in Lower Permian mudstones of the floodplain facies (Figs 9–12) throughout the lower and upper coastal plain and piedmont physiographic provinces (sites 9, 16 and 19 in Fig. 1). Given that these palaeosols are developed in fine-grained mudstones and require good drainage, these palaeosols probably formed upon areas of the floodplains that were removed from frequent flooding and depositional events associated with major stream systems (e.g. Buol *et al.*, 1997).

Interpretation and classification

The clay enrichment, abundant continuous argillans on detrital grains and peds and the non-calcareous matrix in the upper portions of type F profiles are evidence of clay translocation. Translocation is facilitated through leaching of Ca²⁺ from clay exchange sites leading to the development of argillic (Bt) horizons (Franzmeier *et al.*, 1985; Birkeland, 1999). Pedogenic carbonate can precipitate in lower horizons of the profile if soluble minerals are incompletely leached from the soil horizon (Buol *et al.*, 1997). The occurrence of pedogenic carbonates in lower portions of type F palaeosols, coupled with limited development of redoximorphic features and illuviated clays deep within the profile, indicate that these palaeosols formed well above the palaeowater table and were well-drained (cf. Schwert-

mann, 1985, e.g. Kraus & Aslan, 1993). The dark yellowish-brown mudstones with fine-scale branching root structures that cap most type F profiles are interpreted to be organic-rich AB horizons.

The presence of well-differentiated profiles with argillic horizons suggests that type F palaeosols were alfisols (Soil Survey Staff, 1998). Modern alfisols form in humid to subhumid, mid-latitude to subtropical regions that have >75–100 cm of annual precipitation (Strahler & Strahler, 1983; Buol *et al.*, 1997). Given that pedogenic carbonate typically accumulates in soils receiving <70 cm mean annual precipitation in low-latitude regions (McFadden, 1988; Birkeland, 1999; Royer, 1999), carbonate-bearing type F palaeosols may record formation at the subhumid to semi-arid climatic boundary. The predominance of smectite and trace amounts of kaolinite in type F palaeosols is consistent with a subhumid to semi-arid palaeoclimate. In addition, some type F palaeosols are characterized by the development of pedogenic carbonates above or within argillic horizons (polygenetic palaeosols). This superposition of calcic-over-argillic horizons is climatically 'out of phase' and suggests that these type F palaeosols formed under two distinctly different climatic regimes: an earlier, wetter climate that leached carbonate and formed argillic horizons in the profile and a subsequent drier climate that accumulated carbonate and formed calcic horizons in the profile (cf. Soil Survey Staff, 1975; Buol *et al.*, 1997). These polygenetic alfisols are stratigraphically limited to the upper Archer City and Nocona Formations as well as the uppermost Waggoner Ranch Formation between the Maybelle and Lake Kemp Limestones (Fig. 2).

The development of multiple, well-defined horizons, which commonly include superimposed argillic horizons, and the composite nature of these palaeosols record prolonged periods (tens to hundreds of ky) of pedogenesis (cf. Bestland *et al.*, 1997). These characteristics coupled with evidence for well-drained profiles suggest that type F palaeosols developed upon stable landscapes distributed throughout the Early Permian Eastern shelf for which the local groundwater table was relatively deep. Evidence of large, deep fossil roots in type F palaeosols in conjunction with the presence of well-developed argillic horizons and blocky ped structure suggest that woodlands may have developed on such stable areas of the Early Permian alluvial landscape (cf. Mack, 1992).

Type G palaeosols

Description

The type G profile is composed of five well-developed mudstone horizons (Fig. 4G; Table 1) that exhibit wedge-shaped structure defined by clay-coated slickensides (middle three horizons; Fig. 5C and D) and contain stage II carbonate nodules and rhizoliths (upper three horizons; Fig. 5F), although a few other type G palaeosols in the upper Waggoner Ranch Formation may exhibit 50–100 mm thick stage III carbonate accumulations near the bases of the profiles. Redoximorphic features are generally lacking with red hues dominating matrix colours. Sand-filled clastic dykes extend throughout most of the profile (to a depth of 1.4 m). The < 2 µm size fraction in the type profile is dominated by smectite and lesser amounts of kaolinite and mica-like minerals (sericite; Table 1; Fig. 7B).

Type G palaeosols developed in mudstones of the floodplain facies throughout the studied Lower Permian strata (Figs 9, 10 and 12). Their development at numerous sites (sites 7–9, 11–14, 16, 18, 23, 24 and 26–31 in Fig. 1) reflects their widespread distribution in the study area.

Interpretation and classification

Analogous to type D palaeosols, type G palaeosols are interpreted as vertisols based on their well-developed vertic features, their smectite-dominated clay composition and the presence of V-shaped cracks developed to significant profile depths. Type G palaeosols, however, exhibit two major differences from type D palaeosols: (1) accumulation of pedogenic carbonate; and (2) a paucity of redoximorphic features. The lack of redoximorphic features in type G palaeosols indicates that these well-drained profiles formed well above the palaeowater table. Furthermore, the significant carbonate accumulation, including stage II and III carbonate horizons in the profiles, and the presence of deeply penetrating V-shaped clastic-filled dykes require prolonged periods of drying of the profiles and prolonged duration of pedogenesis.

Type H palaeosols

Description

The type profile of pedotype H consists of six moderately to well-developed horizons (Fig. 4H; Table 1) that exhibit medium subangular to coarse angular blocky structure in the upper horizons and wedge-shaped structural aggregates

defined by weakly developed slickensides in the lower half of the profile. Mottling is limited to the lowermost horizons and typically exhibits high chroma. A thick, indurated layer (≥ 150 mm) of stage III carbonate accumulation (= petrocalcic horizon; Soil Survey Staff, 1975, 1998; Machette, 1985) near the top of the profile and extensive development of stage II carbonate nodules and calcareous rhizoliths in lower horizons of the profile (Fig. 5H) help to distinguish the type H palaeosol and its pedotypes from all other carbonate-bearing palaeosols. Hydroxy-interlayered minerals and mica-like minerals with trace amounts of kaolinite and chlorite make up the < 2 µm size fraction in the type profile (Fig. 7C). The type profile has lower clay contents (< 2 µm size fraction in matrix of 22–25%) than all other pedotypes.

Type H palaeosols may occur as compound, cumulate and composite profiles developed in Lower Permian mudstones of the floodplain facies (Figs 9–13). Their occurrence at many sites (sites 7–9, 16–22 and 24–31 in Fig. 1) reflects their widespread distribution in the study area.

Interpretation and classification

Type H palaeosols are interpreted as having been similar to modern aridisols that formed under semi-arid to arid climate conditions based on their extensive carbonate accumulation, in particular as petrocalcic horizons, and relatively low clay contents in comparison with all other pedotypes (Soil Survey Staff, 1998). In reality, these palaeosols may only be classified as inceptisols in the US Soil Taxonomy, as climate conditions are not clearly understood during Early Permian time (Soil Survey Staff, 1998). Nonetheless, the presence of chlorite in the fine clay fraction suggests that type H palaeosols formed under conditions of low soil moisture given that chlorite is not stable in humid environments (cf. Yemane *et al.*, 1996).

Type H palaeosols are interpreted as having formed on infrequently flooded, stable regions of Early Permian floodplains given that they record well-drained and oxidizing soil conditions and that the development of thick petrocalcic horizons requires extended periods of soil formation and soil moisture deficiency (Machette, 1985; Wright & Marriott, 1996). The occurrence of wedge-shaped aggregates defined by weakly developed slickensides in horizons underlying the calcic horizons, however, records fluctuating soil moisture conditions.

DISCUSSION

Permo-Pennsylvanian palaeosols of north-central Texas exhibit clear stratigraphic trends in pedotype distribution and their mineralogical and geochemical compositions. These superimposed trends are interpreted here as recording the interplay of autogenic factors inherent in the depositional system (e.g. variability in sediment accumulation rate and parent material, local topography, variations in floodplain hydrology or soil drainage conditions) and basin- to regional-scale allogenic processes such as climate, tectonic subsidence and eustasy. The overall stratigraphic distribution of the studied palaeosols delineates the time of appearance and disappearance of pedotypes over the Permo-Pennsylvanian interval, as well as defining long-term variations in the inferred degrees of hydromorphy, free drainage and chemical weathering of the soil profiles and estimated soil moisture conditions. These long-term variations are interpreted here as recording the predominant role that climate played in the development of Permo-Pennsylvanian palaeosols associated with the Eastern shelf of the Midland basin. Before discussing the application of these palaeosols to constraining climate over western equatorial Pangea, the role of autogenic and basin-scale allogenic processes other than climate in determining the development of the pedotypes and their observed spatial distribution is first assessed.

Superimposed upon the longer term stratigraphic trend are smaller scale patterns in pedotype distribution defined by palaeosols within thin stratigraphic intervals (metres to a few tens metres; e.g. Fig. 14A and B). Lateral variations in pedotype distribution, degree of maturity of palaeosols and stratigraphic relationships between palaeosols are also observed between age-equivalent deposits located hundreds of metres to tens of kilometres apart (Figs 6, 9, 10, 12 and 13). Reconstruction of palaeocatenas (e.g. fluvial channels and their associated floodplains) in this study was limited to a few laterally continuous outcrops (hundreds of metres to 1.2 km long) exposed along Holocene stream valleys or in badland exposures (e.g. Figs 9 and 13; Tabor, 1999). The observed topography coupled with palaeocatenary relationships inferred from metre-scale vertical stacking patterns of pedotypes indicates that geomorphic position on the aggrading floodplain influenced soil development through differences in topographically controlled drainage and sediment accumulation provided by

channel-margin deposits and shallow floodplain scours (cf. Bown & Kraus, 1987; Kraus, 1986). For the latest Pennsylvanian period, the metre-scale intercalation of type A and type B palaeosols in floodplain strata deposited on the lower palaeo-coastal plain (Figs 6 and 15A) necessitates the presence of topography on the palaeolandscape during pedogenesis. Although both palaeosol types were hydromorphic, the presence of well-developed argillic horizons in type B palaeosols indicates episodic free drainage of these profiles in comparison with the penecontemporaneous water-logged type A palaeosols. However, the shallow depth to the palaeowater table inferred from palaeoplinthites in the ultisols, as well as limited field relationships of channel-filling sandstones and floodbasin strata, indicates that the palaeotopography was probably not greater than a few metres.

Larger scale lateral variations (kilometres to tens of km) defined by differences in the stratigraphic distribution of pedotypes observed within time-equivalent mudstone-dominated intervals bracketed by laterally correlatable, major sand bodies (ss units in Figs 2, 6, 10, 12 and 13) further indicate that the geomorphic position in the Permo-Pennsylvanian alluvial basin influenced soil development, probably through the influence of river channel avulsion and broader patterns of floodplain drainage (cf. Kraus & Aslan, 1993; Kraus, 2002). Overall, these inferred meso- and macroscale palaeosol-landscape associations indicate that differences in sediment accumulation rates and topographically (or parent material) controlled drainage clearly influenced soil development on the Eastern shelf alluvial basin (e.g. Fig. 14B; Sobocki & Wilding, 1983; Wilding *et al.*, 1991; Arndorff, 1993; Bestland *et al.*, 1997; Kraus, 1999, 2002; Kraus & Aslan, 1999). In turn, the imprint of landscape variability is recorded in the vertical stacking patterns of pedotypes at the metre to tens of metre scale and accounts for the stratigraphic 'noise' observed in the longer term trend.

Larger scale (tens to hundreds of metres) stratigraphic variations in the Permo-Pennsylvanian palaeosols define a long-term trend upon which the aforementioned smaller scale variations are superimposed. The long-term trend records an overall decrease in the degree of hydromorphy and intensity of chemical weathering of the soil profiles concomitant with an increase in evidence for free drainage of profiles and lower soil moisture throughout latest Pennsylvanian (Virgilian) to Early Permian time. This trend is defined by

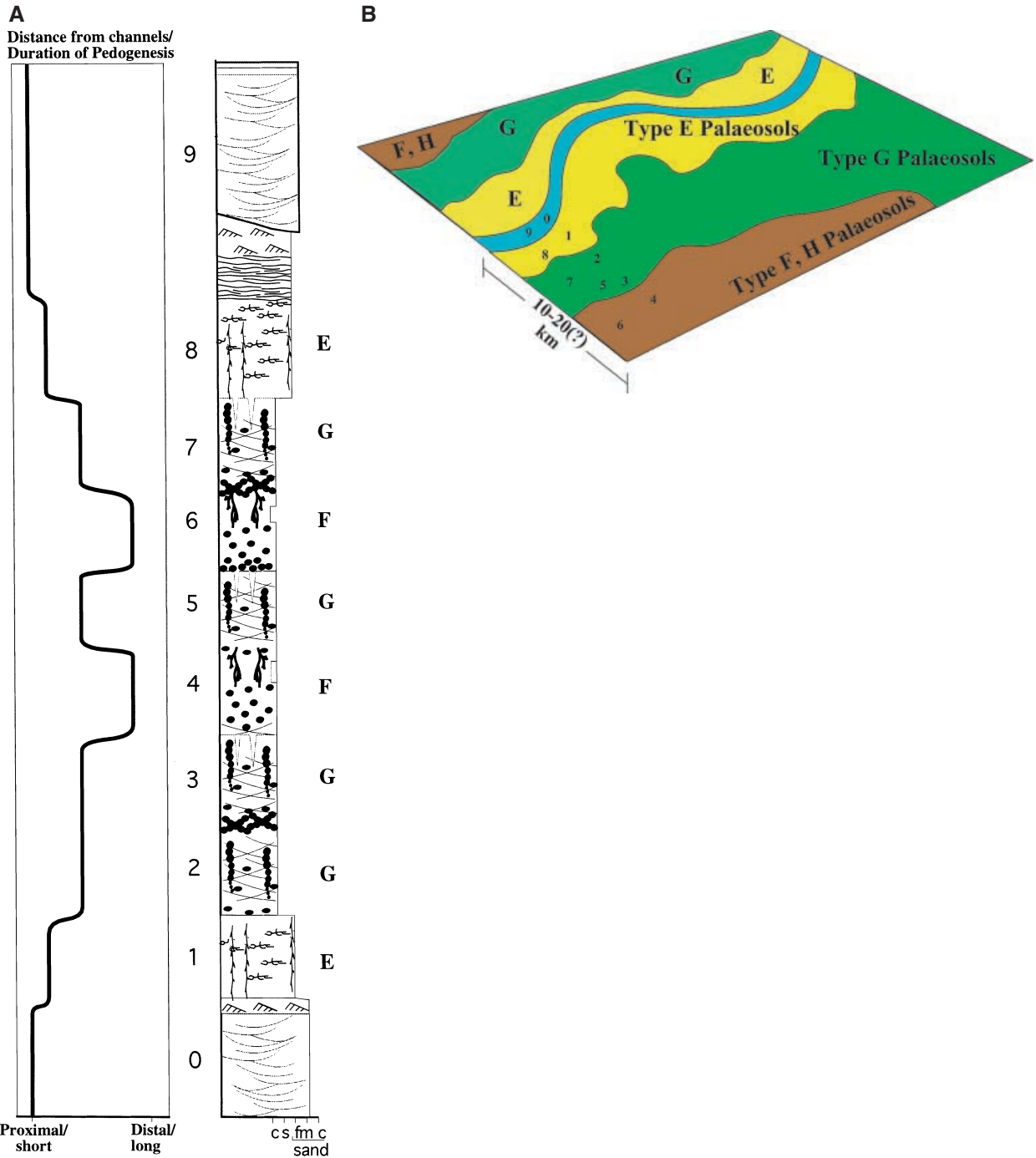


Fig. 14. (A) Schematic stratigraphic column of fluvio-alluvial sedimentary rocks from the Early Permian succession of the Eastern Midland Basin, north-central Texas. The distribution of pedotypes between major fluvial channel deposits suggests that depositional rate, position of the palaeogroundwater table and duration of pedogenesis across the Permo-Pennsylvanian landscape played an important role in the stratigraphic stacking pattern of palaeosol morphologies. (B) Interpreted distribution of soil types across the Early Pennsylvanian landscape of the Eastern Midland Basin, north-central Texas. The stacking pattern of pedotypes between major fluvial channel sandstone deposits is interpreted as representing migration of fluvial systems from proximal (positions 0 and 1) to more distal (positions 4 and 6) and back to proximal locations (positions 8 and 9). See text.

floodplain palaeosols with morphologies that reflect conditions of chemical weathering and soil moisture regime (types A, B, D, F, G and H); no

equivalent trend is defined by the distribution of type C and E profiles (Fig. 15). Type C and E profiles are immature, poorly developed palaeosols

found throughout the three physiographic provinces. Their cosmopolitan nature probably reflects the abundance of young, episodically 'disturbed' and poorly drained environments proximal to fluvial channels and ponds upon the floodplain (Buol *et al.*, 1997).

In particular, the longer term variation in pedotype development records a relatively rapid shift over tens of metres from Late Pennsylvanian hydromorphic floodplain palaeosols (histosol-like type A; ultisol-like type B) to Early Permian well-drained and oxidized profiles (alfisol-like type F; calcic vertisol-like type G; and aridisol-like type H). Vertisols (type D) with abundant redoximorphic features but morphological evidence for periods of drying (e.g. clastic dykes in the upper portions of profiles) make up an important component of latest Pennsylvanian mature palaeosols. These palaeosols are interpreted as recording intermediate soil moisture conditions and the initiation of a drying trend during the transition at the Pennsylvanian–Permian boundary interval.

The Early Permian palaeosols (types F, G and H) record the onset of significant pedogenic carbonate accumulation throughout the region, which could reflect a decrease in average soil moisture levels and/or an increase in Ca^{2+} dust flux to the region. Moreover, a continuum of soil moisture conditions is defined by these three Early Permian pedotypes (alfisols = wettest to aridisols = driest) by the previously discussed differences in their morphologies, abundance and distribution of redoximorphic features and clay composition. Indicators of seasonal or episodic fluctuations in soil moisture conditions occur in all mature palaeosols in the study area except histosols. However, the degree to which the morphological indicators of soil moisture fluctuations and, increasingly, better soil drainage are developed in the studied palaeosols increases significantly from weakly developed features in ultisols of the lower half of the Virgilian strata to strongly developed features in earliest Early Permian alfisols and calcic vertisols.

The stratigraphic distribution of Early Permian pedotypes (F, G and H) does not define a strong temporal trend given that all three pedotypes co-exist in contemporaneous intervals. Type F palaeosols (alfisols), however, become somewhat less abundant upwards through the Early Permian strata (Waggoner Ranch Fm.) with a concomitant increase in the abundance of type H palaeosols (aridisols; Fig. 15).

The longer term trend defined by the studied palaeosols could reflect a change in regional base level governed by tectonic activity or eustasy that may not have been directly linked to climate change (cf. Marriott & Wright, 1993; Wright & Marriott, 1993). The palaeoshoreline migrated north-north-eastward throughout the latest Pennsylvanian to Early Permian in response to a relative sea-level rise, as recorded by the incursion of marine deposits on to the Eastern Shelf (Figs 2 and 14; Hentz, 1988). This shift in base level is expressed in the basinward shift in the geomorphic position of palaeosol-bearing intervals in the studied Permo-Pennsylvanian strata through time (Table 2; Fig. 15). This shift should be recorded by a progressive increase in hydromorphy in response to shallower regional groundwater tables or overall increased maturity of floodplain palaeosols with increasing distance from sediment source areas (Wright & Marriott, 1993; Birkeland, 1999; Kraus, 1999). The observed long-term trend of decreasing degree of hydromorphy and intensity of chemical weathering of the palaeosol profiles concomitant with increasing evidence for free drainage of profiles and overall falling soil moisture levels, however, is contrary to the trends anticipated in response to a rise in base level. This indicates the predominant influence of an allogenic process(es) other than base level on the observed long-term trend in pedotype distribution. However, the greater abundance of type G (calcic vertisols) and type F (alfisols) on landscapes proximal to the palaeoshoreline (0 to \approx 30 km; Table 2) and a dominance of aridisols (type H) in regions of the alluvial basin proximal to sediment sources (> 60 km from base level; Table 2) does indicate that a decline in topographic relief and sediment accumulation rates down palaeoslope on the Eastern Shelf may have had a subordinate influence on the observed larger scale stratigraphic variations in palaeosol morphology and maturity. The weak manifestation of these basin-wide trends, however, attests to the very low palaeoslopes on the Late Palaeozoic Eastern shelf. Temporal variation in Permo-Pennsylvanian parent material in the study area as an alternative allogenic control on the large-scale stratigraphic variations in pedotype is not considered likely given the lack of any observed systematic long-term variation in parent material derived from the Ouachita or Arbuckle uplands (Hentz, 1988).

It is suggested that climate was the predominant control on the origin of large-scale stratigraphic variations in pedotype distribution in

Table 2. Relationship of Permo-Pennsylvanian palaeosol sites relative to estimated base-level on the Eastern shelf of the Midland Basin.

Formation	Distance from relative sea level and palaeosol morphology*												
	0–10 km	10–20 km	20–30 km	30–40 km	40–50 km	50–60 km	> 60 km	Site #	Type	Site #	Type	Site #	Type
Waggoner Ranch	31	H,F,G	26	H,G,I	29	H,G	30	H',E'	-	-	-	-	-
	-	-	27	H,G,I	-	-	-	-	-	-	-	-	-
	-	-	28	H,G,E	-	-	-	-	-	-	-	-	-
Petrolia	-	-	-	-	25	H,E	-	-	-	-	-	-	-
	-	-	-	-	24	H,E,G	-	-	-	-	-	-	-
	23	G'	-	-	-	-	-	-	-	-	-	-	19
Nocona	-	-	22	H,F,G,E	-	-	-	-	-	-	-	-	-
	-	-	-	-	-	-	-	-	-	-	-	-	20
	-	-	-	-	-	-	-	-	-	-	-	-	21
Archer City	-	-	18	H	-	-	-	-	-	-	-	-	-
	-	-	17	H,F	-	-	-	-	-	-	-	-	-
	-	-	16	H,G,F,E	-	-	-	-	-	-	-	-	14
Markley	-	-	-	-	-	-	-	-	-	-	-	-	15
	-	-	-	-	-	-	-	-	-	-	-	-	13
	-	-	-	-	12	G,E	-	-	-	-	-	-	-
	-	-	-	-	-	-	9	G,H,F,E	-	-	-	-	-
	-	-	-	-	-	-	10	H,G	-	-	-	-	-
	-	-	-	-	-	-	11	G,H	-	-	8	G,H	-
-	-	-	-	-	-	-	-	-	7	G,E	-	-	
-	-	-	-	-	-	-	-	-	-	-	1	A,B,C	
-	-	-	-	-	-	-	-	-	-	-	2	A,B,C	
-	-	-	-	-	-	-	-	-	-	-	3	A	
-	-	-	-	-	-	-	-	-	-	-	4	C	
-	-	-	-	-	-	-	-	-	-	-	5	C,E	
-	-	-	-	-	-	-	-	-	-	-	6	C,D,E	

* The distance from base level was determined by measuring the distance down depositional dip from the study sites to the vertically dashed lines in Fig. 2 that represent the stratigraphic cut-off between marine-dominated and terrestrial-dominated sedimentary strata (Hentz, 1988). These are likely to be minimum estimates, as soil formation occurred on the floodplains during times of base level fall or lowstand (e.g. mid-continent cyclothem). The position of each of the study sites and their associated palaeosol morphologies are given in relation to (1) distance from base level (inferred from dashed lines in Fig. 2); and (2) stratigraphic occurrence. The purpose of this table is to assess the distribution of palaeosols relative to base level. Although more data should be gathered to test rigorously the effects of base level (and base level change) on the morphology of palaeosols in the study area, it is apparent that there is no robust change in palaeosol morphology as a function of distance from base level for any one time period.

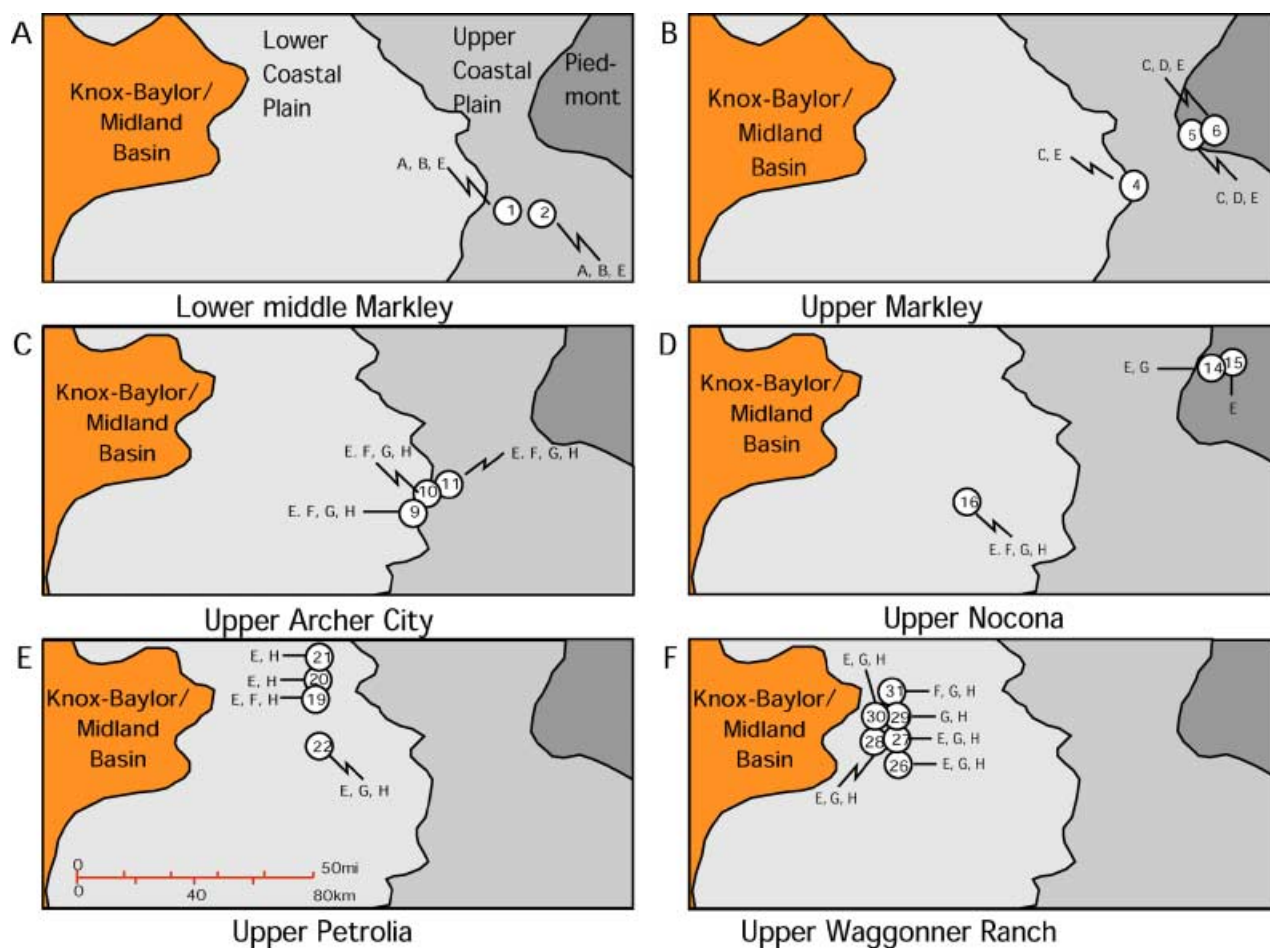


Fig. 15. Schematic diagram of the Permo-Pennsylvanian landscape through time based on palaeosol morphological features. Roughly contemporaneous study sites from Figs 1 and 2 are plotted on each time period, as well as the palaeosol types associated with each study site. See text for discussion.

the study area. The Late Palaeozoic is hypothesized to have been characterized by major changes in climate in response to the assembly of the supercontinent Pangea, a transition from ice-house to green-house states and major changes in atmospheric circulation (Veevers & Powell, 1987; Parrish, 1993; Crowley, 1994). Climatically sensitive depositional and palaeontological records for low-latitude Pangea (Rowley *et al.*, 1985; Cecil, 1990; Dubiel *et al.*, 1991; DiMichele & Aronson, 1992; Parrish, 1993; West *et al.*, 1997; Kessler *et al.*, 2001; Rees *et al.*, 2001) coupled with numerical model results (Parrish *et al.*, 1986; Kutzbach & Gallimore, 1989; Patzkowsky *et al.*, 1991; Gibbs *et al.*, 2002) suggest that the mid-latitude and equatorial regions of Pangea became progressively more arid and seasonal throughout the Late Palaeozoic. The long-term aridification trend has been attributed to several processes including: (1) northward drift of

Pangea out of the Intertropical Convergence Zone into the more arid low-latitude belt; (2) rain shadow effects created by uplift of the Alleghenian and Ouachita mountains; and (3) northward diversion of moisture-laden easterlies by the development of northern hemisphere monsoonal circulation.

Significantly, recent studies have suggested that monsoonal circulation and attendant westerly winds were well-established over western equatorial Pangea by earliest Permian time (Kessler *et al.*, 2001; Soreghan, G.S. *et al.*, 2002; Soreghan, M.J. *et al.*, 2002; Tabor & Montañez, 2002; Loope *et al.*, 2004), despite model results indicating that continental-scale monsoonal circulation would have strengthened progressively to its peak in the Middle Triassic (Parrish, 1993). The results of these lithological and geochemical studies, along with other discrepancies in model-data comparisons for low-latitude western Pangea

(Patzkowsky *et al.*, 1991; Rees *et al.*, 2001; Gibbs *et al.*, 2002), highlight the need for a better understanding of specific climate zones over Late Palaeozoic Pangea. Pennsylvanian to Permian palaeosols from north-central Texas provide additional constraints on the nature and origin of climate change over low-latitude Pangea given that climate change would have been most pronounced in western equatorial Pangea (Dubiel *et al.*, 1991; Parrish, 1993).

The long-term variation in soil moisture conditions and, in turn, precipitation inferred from the large-scale stratigraphic variations in Permo-Pennsylvanian pedotypes confirms the previously defined long-term aridification trend for western equatorial Pangea. Notably, however, the palaeosol data in this study indicate that the long-term drop in inferred soil moisture levels accelerated at end-Pennsylvanian time. Incipient morphological indicators of seasonality preserved in type D palaeosols of the study area suggest an abrupt onset of seasonality in conjunction with a rapid decline in net soil moisture budget in the latest Pennsylvanian.

The long-term aridification trend inferred from the palaeosol data cannot be interpreted as reflecting northward drift of Pangea given that palaeomagnetic studies indicate that the area remained within a few degrees of the equator throughout the Early Permian (Scotese, 1999; Loope *et al.*, 2004). The observed temporal trend may record the development of a rain shadow in western Pangea in response to uplift of the equatorial Alleghenian and Ouachita mountains (Rowley *et al.*, 1985; Parrish, 1993; Ziegler *et al.*, 1997). However, the degree to which long-term aridification through the latest Pennsylvanian and Early Permian can be explained by a rain shadow effect is strongly dependent on the elevation of the equatorial highlands, for which a significant degree of uncertainty exists (Otto-Bliesner, 1993, 1998; Fluteau *et al.*, 2001; Gibbs *et al.*, 2002). Moreover, the orographic effect of these prominent equatorial highlands on tropical precipitation (i.e. onset of aridity) should have been well-established by Late Carboniferous time rather than in the Early Permian as the palaeosols of the Eastern shelf suggest (cf. Kessler *et al.*, 2001; Soreghan G.S. *et al.*, 2002).

The overall long-term palaeopedogenic trend and its inferred rapid decline in precipitation levels and intensification of seasonality in western equatorial Pangea in the latest Pennsylvanian and earliest Permian are strong evidence for northern hemisphere monsoonal circulation. For

western equatorial Pangea, this rapid change in regional climatic conditions may record a tectonic moderation of monsoonal conditions. Uplift of the equatorial mountain chain in the Early Pennsylvanian (Chesterian) would have acted to intensify the normal low pressure area of the equatorial belt, thus inhibiting the development of fully monsoonal conditions until their erosion in the latest Pennsylvanian and Early Permian dampened their climatic influence (Rowley *et al.*, 1985; Otto-Bliesner, 1993). Notably, the delay in the development of fully monsoonal conditions may have promoted relatively rapid intensification of monsoonal conditions over the study area in the Early Permian as has been invoked to explain the origin of rapid variation in lithofacies of mid-continent cyclothem in the latest Pennsylvanian to earliest Permian (West *et al.*, 1997).

Lastly, pedogenic evidence for intermediate-scale (10^3 – 10^5 years) climate fluctuations in western equatorial Pangea occurs in the polygenetic alfisols characterized by well-developed calcic horizons overlying or superimposed on argillic horizons. These polygenetic palaeosols are restricted stratigraphically to the lower half of Lower Permian (Wolfcampian) deposits of north-central Texas, and reappear for a few tens of metres in the uppermost Leonardian-age Waggoner Ranch and lowermost Clear Fork Formations. These polygenetic profiles are analogous to those that occur within slightly younger, Lower Permian mid-continent cyclothem that have been interpreted to record orbitally forced ≈ 20 ky climate oscillations associated with waxing and waning of Early Permian continental glaciers (Miller *et al.*, 1996). Such precessional forcing of climate would probably have been dampened following deglaciation and a transition to greenhouse states. If polygenetic palaeosols from the eastern Midland basin record precessional-scale climate fluctuations, then the abrupt shift to more stable climatic conditions marked by the loss of polygenetic palaeosols in the Early Permian (mid-Leonardian) succession may be a sensitive record of the onset of deglaciation. The brief reappearance of polygenetic alfisols in the later part of the Early Permian might record a brief renewed episode of glaciation or a climatic cooling analogous to the late Quaternary Younger Dryas. This interpretation, if correct, places additional constraints on most recent estimates of a late Early Permian age for the onset of deglaciation (Veevers, 1994; Gibbs *et al.*, 2002).

CONCLUSIONS

Late Pennsylvanian and Early Permian sedimentary strata of the Eastern Midland basin exhibit a change in palaeosol morphological, mineralogical and chemical characters across the Pennsylvanian–Permian boundary. This change is revealed by palaeosols with well-developed redoximorphic depletions and concentrations in the Late Pennsylvanian that are replaced by palaeosols that generally lack redoximorphic indicators in the Early Permian. Furthermore, many of the Early Permian palaeosols are characterized by pedogenic carbonate accumulation that is consistent with a net soil moisture deficiency, whereas Late Pennsylvanian palaeosols exhibit no pedogenic carbonate. The clay mineralogical composition of these palaeosols indicates a change from more highly weathered and probably humid conditions in the Late Pennsylvanian to less extreme weathering and potentially semi-arid to arid conditions in the Early Permian. These changes may be a response to changing soil moisture regimes from humid, poorly drained to dry, well-drained conditions in the Late Pennsylvanian to Early Permian.

The inferred change in Late Pennsylvanian–Early Permian soil moisture regimes of western equatorial Pangea is likely to be related to climate change. It is suggested, based on the preserved lithological, mineralogical and chemical characteristics of these palaeosols, that a change occurred from a humid tropical climate characterized by high rainfall in the Pennsylvanian to a progressively drier tropical climate characterized by seasonal precipitation throughout the Early Permian. Furthermore, these data indicate the onset of monsoonal-type precipitation patterns nearly coincident with the Pennsylvanian–Permian boundary. Although these strata preserve a general trend of progressively drier and seasonal precipitation through the Permian, polygenetic soils preserved within the lower half of the Early Permian (Wolfcampian) and uppermost strata of the lower Leonardian Waggoner Ranch Formation may indicate an oscillatory climate pattern between more humid and drier climate during deposition of these stratigraphic packages

ACKNOWLEDGEMENTS

We are deeply indebted to Bill DiMichele and Dan Chaney, Department of Palaeobiology, Museum of Natural History, Smithsonian Institution, for

providing an introduction to the study area. John Nelson and Dan Chaney provided excellent field guidance. This project was funded by NSF grant EAR-9814640 to I. P. Montanez and an NSF-IGERT graduate fellowship to N. J. Tabor. Funding was also provided by grants to N.J.T. from the Geological Society of America, American Association of Petroleum Geologists, Society for Sedimentary Geology and Sigma Xi. We thank Peter Houghton, Paul McCarthy and Susan Marriott for their thoughts and helpful comments on this manuscript. All these reviewers (but particularly S.M.) have contributed significantly towards improving the quality and clarity of this contribution.

REFERENCES

- Arndorff, L.** (1993) Calcretes from Hollviken-II drill core, Skane, southern Sweden. In: *Lundadagarna I; Historical Geology and Paleontology* (Ed. M. Siverson), *Lund Publ. Geol.*, **109**, 3.
- Barnes, V.E., Hentz, T.F. and Brown, L.F., Jr** (1987) *Geologic Atlas of Texas; Wichita Falls – Lawton Sheet*. University of Texas at Austin, Bureau of Economic Geology, Austin, TX.
- Bein, A. and Land, L.** (1983) Carbonate sedimentation and diagenesis associated with Mg-Ca-chloride brines; the Permian San Andres Formation in the Texas panhandle. *J. Sed. Petrol.*, **53**, 243–260.
- Bestland, E.A., Retallack, G.J. and Swisher, C.C., III** (1997) Stepwise climate change recorded in Eocene-Oligocene paleosol sequences from central Oregon. *J. Geol.*, **105**, 153–172.
- Birkeland, P.W.** (1999) *Soils and Geomorphology*, 3rd edn. Oxford University Press, New York, 430 pp.
- Bown, T.M. and Kraus, M.J.** (1987) Integration of channel and floodplain suites. I. Developmental sequence and lateral relations of alluvial paleosols. *J. Sed. Petrol.*, **57**, 587–601.
- van Breeman, N. and Harmsen, K.** (1975) Translocation of iron in acid sulfate soils; I, soil morphology and the chemistry and mineralogy of iron in a chronosequence of acid sulfate soils. *Soil Sci. Soc. Am.*, **39**, 1140–1147.
- Brewer, R.** (1976) *Fabric and Mineral Analysis of Soils*. Krieger, New York, 482 pp.
- Brown, L.F., Jr** (1973) Pennsylvanian rocks of North-Central Texas: an introduction. In: *Pennsylvanian Depositional Systems in North-Central Texas* (Ed. L.F. Brown, Jr), *Bur. Econ. Geol. Guidebook*, **14**, 1–9.
- Brown, L.F., Jr Solis Irarte, R.F. and Johns, D.A.** (1987) *Regional Stratigraphic Cross Sections, Upper Pennsylvanian and Lower Permian Strata (Virgilian and Wolfcampian Series), North-central-Central Texas*. Bureau of Economic Geology, University of Texas at Austin, Austin, TX, 27 pp.
- Buol, S.W., Hole, F.D., McCracken, R.J. and Southard, R.J.** (1997) *Soil Genesis and Classification*. Iowa State University Press, Ames, IA, 527 pp.
- Cecil, C.B.** (1990) Paleoclimate controls on stratigraphic repetition of chemical and siliciclastic rocks. *Geology*, **18**, 533–536.
- Crowley, T.J.** (1994) Pangean climates. In: *Pangea: Paleoclimate, Tectonics, and Sedimentation During Accretion, Zenith, and Breakup of a Supercontinent* (Ed. G.D. Klein), *Geol. Soc. Am. Spec. Paper*, **288**, 25–40.

- Daniels, R.B., Gamble, E.E. and Nelson, L.A.** (1971) Relations between soil morphology and water table levels on a dissected North-central Carolina coastal plain surface. *Soil Sci. Soc. Am. Proc.*, **35**, 157–175.
- Deutz, P., Montañez, I.P. and Monger, H.C.** (2002) Morphologies and stable and radiogenic isotope compositions of pedogenic carbonates in Late Quaternary relict and buried soils, New Mexico: an integrated record of pedogenic overprinting. *J. Sed. Res.*, **72**, 809–822.
- DiMichele, W.A. and Aronson, R.B.** (1992) The Pennsylvanian-Permian vegetational transition: a terrestrial analogue to the onshore-offshore hypothesis. *Evolution*, **46**, 807–824.
- Dixon, J.B. and Skinner, H.C.W.** (1992) Manganese minerals in surface environments. *Catena Suppl.*, **21**, 31–50.
- Donovan, R.N., Collins, K. and Bridges, S.** (2001) Permian sedimentation and diagenesis on the Northern Margin of the Wichita uplift. *Okl. Geol. Surv. Circ.*, **104**, 171–184.
- Dubiel, R.F., Parrish, J.T., Parrish, J.M. and Good, S.C.** (1991) The Pangean megamonsoon – evidence from the Upper Triassic Chinle Formation, Colorado Plateau. *Palaios*, **6**, 347–370.
- Duchaufour, P.** (1982) *Pedology: Pedogenesis and Classification*. George Allen & Unwin, London, 448 pp.
- Dudal, R. and Eswaran, H.** (1988) Chapter 1: Distribution, properties and classification of Vertisols. In: *Vertisols: Their Distribution, Properties, Classification and Management* (Eds L.P. Wilding and R. Puentes), pp. 1–22. Texas A&M University Publishing Center, College Station, TX.
- Dunbar, C.O. and Committee on Stratigraphy** (1960) Correlation of the Permian formations of North-central America. *Geol. Soc. Am. Bull.*, **71**, 1763–1806.
- Fanning, D.S. and Fanning, M.C.B.** (1989) *Soil: Morphology, Genesis, and Classification*. Wiley and Sons, New York, 395 pp.
- Fluteau, F., Besse, J., Broutin, J. and Ramstein, G.** (2001) The Late Permian climate. What can be inferred from climate modeling concerning Pangea scenarios and Hercynian range altitude? *Palaeogeogr. Palaeoclimatol. Palaeoecol.*, **167**, 39–71.
- Franzmeier, F.P., Bryant, R.B. and Steinhardt, G.C.** (1985) Characteristics of Wisconsinan glacial tills in Indiana and their influence on Argillic horizon development. *Soil Sci. Soc. Am. J.*, **49**, 1481–1486.
- Gibbs, M.T., Rees, P.M., Kutzbach, J.E., Ziegler, A.M., Behling, P.J. and Rowley, D.B.** (2002) Simulations of Permian climate and comparisons with climate-sensitive sediments. *J. Geol.*, **110**, 33–55.
- Gill, S. and Yemane, K.** (1996) Implications of a Lower Pennsylvanian Ultisol for equatorial Pangean climates and early oligotrophic forest ecosystems. *Geology*, **24**, 905–908.
- Golonka, J., Ross, M.I. and Scotese, C.R.** (1994) Phanerozoic paleogeographic and paleoclimatic modeling maps. In: *Pangea: Global Environments and Resources* (Eds A.F. Embry, B. Beauchamp and D.J. Glass), *Can. Soc. Petrol. Geol. Mem.*, **17**, 1–47.
- Hentz, T.F.** (1988) Lithostratigraphy and paleoenvironments of Upper Paleozoic continental red beds, north-central-central Texas: Bowie (new) and Wichita (revised) Groups. *Bur. Econ. Geol. Report Invest.*, **170**, 49 pp.
- Jim, C.Y.** (1990) Stress, shear deformation and micromorphological clay orientation: a synthesis of various concepts. *Catena*, **17**, 431–447.
- Kessler, J.L.P. and Soreghan, G.S. and Wacker, H.J.** (2001) Equatorial aridity in western Pangea: Lower Permian loessite and dolomitic paleosols in northeastern New Mexico, USA. *J. Sed. Res.*, **71**, 817–832.
- Kraus, M.J.** (1986) Integration of channel and floodplain suites II. Vertical relations of alluvial paleosols. *J. Sed. Petrol.*, **57**, 602–612.
- Kraus, M.J.** (1998) Development of potential acid sulfate paleosols in Paleocene floodplains, Bighorn Basin, Wyoming USA *Palaeogeogr. Palaeoclimatol. Palaeoecol.*, **144**, 203–224.
- Kraus, M.J.** (1999) Paleosols in clastic sedimentary rocks: their geologic significance. *Earth-Sci. Rev.*, **47**, 41–70.
- Kraus, M.J.** (2002) Basin-scale changes in floodplain paleosols: implications for interpreting alluvial architecture. *J. Sed. Petrol.*, **72**, 500–509.
- Kraus, M.J. and Aslan, A.** (1993) Eocene hydromorphic paleosols: significance for interpreting ancient floodplain processes. *J. Sed. Petrol.*, **63**, 453–463.
- Kraus, M.J. and Aslan, A.** (1999) Paleosol sequences in floodplain environments: a hierarchical approach. In: *Palaeoweathering, Palaeosurfaces and Related Continental Deposits*. (Ed. M. Thiry), *Int. Assoc. Sedimentol. Spec. Publ.*, **27**, 303–321.
- Kutzbach, J.E. and Gallimore, R.G.** (1989) Pangean climates: megamonsoons of the megacontinent. *J. Geophys. Res.*, **94**, 3341–3357.
- Loope, D.B., Steiner, M.B. and Rowe, C.M.** (2004) Tropical westerlies over Pangean sand seas. *Sedimentology*, **51**, 315–322.
- McFadden, L.D.** (1988) Climatic influences on rates and processes of soil development in Quaternary deposits of Southern California. In: *Paleosols and Weathering Through Time; Principles and Applications* (Eds J. Reihardt and W.R. Sigleo), *Geol. Soc. Am. Spec. Publ.*, **216**, 153–177.
- McGowen, J.H., Granata, G.E. and Seni, S.J.** (1979) Depositional framework of the Lower Dockum Group (Triassic) Texas Panhandle. *Bur. Econ. Geol. Report Invest.*, **97**, 60 pp.
- Machette, M.N.** (1985) Calcic soils of southwestern United States. *Geol. Soc. Am. Spec. Paper*, **203**, 1–21.
- Mack, G.H.** (1992) Paleosols as an indicator of climatic change at the Early–Late Cretaceous boundary, southwestern New Mexico. *J. Sed. Petrol.*, **62**, 483–494.
- Markewich, H.W. and Pavich, M.J.** (1991) Soil chronosequence studies in temperate to subtropical, low-latitude, low relief terrain with data from the eastern United States. *Geoderma*, **51**, 213–239.
- Marriott, S.B. and Wright, V.P.** (1993) Paleosols as indicators of geomorphic stability in two Old Red Sandstone alluvial suites, South Wales. *J. Geol. Soc. London*, **150**, 1109–1120.
- Miller, K.B., McCahon, T.J. and West, R.R.** (1996) Lower Permian (Wolfcampian) paleosol-bearing cycles of the US midcontinent; evidence of climatic cyclicity. *J. Sed. Res.*, **66**, 71–84.
- Munsell Color** (1975) *Munsell Soil Color Charts*. Munsell Color, Baltimore, MD, 24 pp.
- Nelson, W.J., Hook, R.W. and Tabor, N.J.** (2001) Clear Fork Group (Leonardian, Lower Permian) of North-Central Texas. *Okl. Geol. Surv. Circ.*, **104**, 167–169.
- Oriel, S., Myers, D.A. and Crosby, E.J.** (1967) Paleotectonic investigations of the Permian system in the United States. *US Geol. Surv. Prof. Paper*, **515**, Chapter C, 80 pp.
- Otto-Bliesner, B.L.** (1993) Tropical mountains and coal formation: a climate model study of the Westphalian (306 MA). *Geophys. Res. Lett.*, **20**, 1947–1950.
- Otto-Bliesner, B.L.** (1998) Effects of tropical mountain elevations on the climate of the Late Carboniferous: Climate model simulations. In: *Tectonic Boundary Conditions for Climate Reconstructions* (Eds T.J. Crowley and K.C. Burke), *Oxford Monogr. Geol. Geophys.*, **39**, 100–115.

- Parrish, J.T.** (1993) Climate of the supercontinent Pangea. *J. Geol.*, **101**, 215–233.
- Parrish, J.M., Parrish, J.T. and Ziegler, A.M.** (1986) Permian-Triassic paleogeography and paleoclimatology and implications for therapsid distribution. In: *The Ecology and Biology of Mammal-Reptiles* (Eds N. Hotton, P.D. MacLean, J.J. Roth and C. Roth), pp. 109–131. Smithsonian Institution Press, Washington, DC.
- Patzkowsky, M.E., Smith, L.H., Markwick, P.J., Engberts, C.J. and Gyllenhaal, E.D.** (1991) Application of the Fujita-Ziegler paleoclimate model: Early Permian and Late Cretaceous examples. *Palaeogeogr. Palaeoclimatol. Palaeoecol.*, **86**, 67–85.
- Rasbury, E.T., Hanson, G.N., Meyers, W.J., Holt, W.E., Goldstein, R.H. and Saller, A.H.** (1998) U-Pb dates of paleosols; constraints on late Paleozoic cycle durations and boundary ages. *Geology*, **26**, 403–406.
- Rees, P.M., Ziegler, A.M., Gibbs, M.T., Kutzbach, J.E., Behling, P.J. and Rowley, D.B.** (2001) Permian phytogeographic patterns and climate data/model comparisons. *J. Geol.*, **110**, 1–31.
- Retallack, G.J.** (1988) Field recognition of paleosols. In: *Paleosols and Weathering Through Geologic Time: Principles and Applications* (Eds J. Reinhardt and W.R. Sigleo), *Geol. Soc. Am. Spec. Paper*, **216**, 1–20.
- Retallack, G.J.** (1990) *Soils of the Past: An Introduction to Paleopedology*. Unwin-Hyman, Boston, 520 pp.
- Retallack, G.J.** (1994) A pedotype approach to latest Cretaceous and earliest Tertiary paleosols in eastern Montana. *Geol. Soc. Am. Bull.*, **106**, 1377–1397.
- Retallack, G.J. and German-Heins, J.** (1994) Evidence from paleosols for the geological antiquity of rain forest. *Science*, **265**, 499–502.
- Ross, C.A., Baud, A. and Menning, M.** (1994) A timescale for project Pangea. In: *Pangea; Global Environments and Resources* (Eds B. Beauchamp and D.J. Glass), *Can. Soc. Petrol. Geol. Mem.*, **17**, 81–83.
- Rowley, D.B., Raymond, A., Parrish, J.T., Lottes, A.L., Scotese, C.R. and Ziegler, A.M.** (1985) Carboniferous paleogeographic, phytogeographic, and paleoclimatic reconstructions. *Int. J. Coal Geol.*, **5**, 7–42.
- Royer, D.L.** (1999) Depth to pedogenic carbonate horizon as a paleoprecipitation indicator? *Geology*, **27**, 1123–1126.
- Schwertmann, U.** (1985) Occurrence and formation of iron oxides in various pedoenvironments. In: *Iron in Soils and Clay Minerals* (Eds J.W. Stucki, B.A. Goodman and U. Schwertmann), *NATO Adv. Study Inst. Series C*, **217**, 267–308.
- Scotese, C.R.** (1999) *PALEOMAP Animations 'Paleogeography'*. *PALEOMAP Project*. Department of Geology, University of Texas, Arlington, TX.
- Simonson, G.H. and Boersma, L.** (1972) Soil morphology and water table relations. II. Correlation between annual water table fluctuations and profile features. *Soil Sci. Soc. Am. Proc.*, **36**, 649–653.
- Sobecki, T.M. and Wilding, L.P.** (1983) Calcic horizon distribution and soil classification in selected soils of the Texas Coast Prairie. *Soil Sci. Soc. Am. Proc.*, **46**, 1222–1227.
- Soil Survey Staff** (1975) *Soil Taxonomy*. US Department of Agriculture Handbook, **436**, 754 pp.
- Soil Survey Staff** (1998) *Keys to Soil Taxonomy*. US Department of Agriculture Natural Resources Conservation Service, Washington, DC, 325 pp.
- Soreghan, G.S., Elmore, R.D. and Lewchuk, M.T.** (2002) Sedimentologic-magnetic record of western Pangean climate in upper Paleozoic loessite (lower Cutler beds, Utah). *Geol. Soc. Am. Bull.*, **114**, 1019–1035.
- Soreghan, M.J., Soreghan, G.S. and Hamilton, M.A.** (2002) Paleowinds inferred from detrital-zircon geochronology of upper Paleozoic loessite, western equatorial Pangea. *Geology*, **30**, 695–698.
- Strahler, A.N. and Strahler, A.H.** (1983) *Modern Physical Geography*, 2nd edn. John Wiley and Sons, New York, 532 pp.
- Tabor, N.J.** (1999) Permo-Pennsylvanian alluvial paleosols (north-central Texas): high-resolution proxy records of the evolution of early Pangean Paleoclimate. Unpubl. Master's Thesis, University of California, 121 pp.
- Tabor, N.J. and Montañez, I.P.** (2002) Shifts in late Paleozoic atmospheric circulation over western equatorial Pangea: Insights from pedogenic mineral $\delta^{18}\text{O}$ compositions. *Geology*, **30**, 1127–1130.
- Veevers, J.J.** (1994) Pangea. Evolution of a supercontinent and its consequences for earth's paleoclimate and sedimentary environments. In: *Pangea: Paleoclimate, Tectonics, and Sedimentation During Accretion, Zenith, and Breakup of a Supercontinent* (Ed. G.V. Klein), *Geol. Soc. Am. Spec. Paper*, **288**, 13–23.
- Veevers, J.J. and Powell, M.** (1987) Late Paleozoic glacial episodes in Gondwanaland reflected in transgressive-regressive depositional sequences in Euramerica. *Geol. Soc. Am. Bull.*, **98**, 574–487.
- Vepraskas, M.J.** (1994) Redoximorphic features for identifying aquic conditions. *NC Agric. Res. Service Tech. Bull.*, 301 pp.
- West, R.R., Archer, A.W. and Miller, K.B.** (1997) The role of climate in stratigraphic patterns exhibited by Late Paleozoic rocks exposed in Kansas. *Palaeogeogr. Palaeoclimatol. Palaeoecol.*, **128**, 1–16.
- Wilding, L.P. and Tessier, D.** (1988) Genesis of vertisols: shrink-swell phenomena. In: *Vertisols: Their Distribution, Properties, Classification and Management* (Eds L.P. Wilding and R. Puentes), pp. 55–81. Texas A&M University Publishing Center, College Station, TX.
- Wilding, L.P., Milford, M.H. and Vepraskas, M.J.** (1983) Micromorphology of deeply weathered soils in the Texas Gulf Coast Plains. In: *Soil Micromorphology, Vol. 2* (Eds P. Bullock and C.P. Murphy), pp. 567–574. AB Academic Publishers, Hertfordshire.
- Wilding, L.P., Williams, D., Cook, T., Miller, W. and Eswaran, H.** (1991) Close interval spatial variability of vertisols: a case study in Texas. *Proceedings of the Sixth International Soil Correlation Meeting*, pp. 232–247. US Department of Agriculture – Soil Conservation Service, Washington, DC.
- Wright, V.P.** (1990) A micromorphological classification of fossil and recent calcic and petrocalcic microstructures. *Proc. Int. Working Meeting Soil Micromorphol.*, **8**, 401–407.
- Wright, V.P. and Marriott, S.B.** (1993) The sequence stratigraphy of fluvial depositional systems: the role of floodplain sediment storage. *Sed. Geol.*, **86**, 203–210.
- Wright, V.P. and Marriott, S.B.** (1996) A quantitative approach to soil occurrence in alluvial deposits and its application to the Old Red Sandstone of Britain. *J. Geol. Soc. London*, **153**, 907–913.
- Yaalon, D.H. and Kalmar, D.** (1978) Dynamics of cracking and swelling clay soils: displacement of skeletal grains, optimum depth of slickensides, and rate of intra-pedonic turbation. *Earth Surf. Proc.*, **3**, 31–42.

Yemane, K., Kahr, G. and Kelts, K. (1996) Imprints of post-glacial climates and paleogeography in the detrital clay mineral assemblages of an Upper Permian fluviolacustrine Gondwana deposit from north-central Malawi. *Palaeogeogr. Palaeoclimatol. Palaeoecol.*, **125**, 27–49.

Ziegler, A.M., Hulver, M.L. and Rowley, D.B. (1997) Permian World Topography and Climate. In: *Late Glacial and*

Postglacial Environmental Changes – Pleistocene, Carboniferous-Permian and Proterozoic (Ed. I.P. Martini), pp. 111–146. Oxford University Press, Oxford.

*Manuscript received 2 July 2003;
revision accepted 22 March 2004.*

Copyright of Sedimentology is the property of Blackwell Publishing Limited and its content may not be copied or emailed to multiple sites or posted to a listserv without the copyright holder's express written permission. However, users may print, download, or email articles for individual use.